Real-time RT-PCR analysis

Total cellular RNA was extracted from cultured cells or liver tissue using ISOGEN (Nippon Gene, Tokyo, Japan). Total cellular RNA (2 μg) was used to generate cDNA from each sample using the SuperScript II reverse-transcriptase (Invitrogen). The mRNA expression levels were measured using the Light Cycler PCR and detection system (Roche, Mannheim, Germany) and Light Cycler Fast Start DNA Master SYBR Green 1 mix (Roche).

Luciferase assays

Luciferase activity was measured using a luminometer, Lumat LB9501 (Promega) and the Bright-Glo Luciferase Assay System (Promega) or the Dual-Luciferase Reporter Assay System (Promega).

Northern and western hybridization

Total cellular RNA was separated by denaturing agarose-formaldehyde gel electrophoresis, and transferred to a nylon membrane. The membrane was hybridized with a digoxigenin-labeled probe specific for the full-length replicon sequence, and subsequently with a probe specific for beta-actin. The signals were detected by chemiluminescence reaction using a Digoxigenin Luminescent Detection Kit (Roche), and visualized by Fluoro-Imager (Roche). For the western blotting, 10 μg of total cell lysate was separated on NuPAGE 4.12% Bis-TrisGel (Invitrogen), and blotted onto an Immobilon PVDF Membrane (Roche). The membrane was incubated with monoclonal antibodies specific for HCV-NS5A (BioDesign, Saco, ME, USA), NS4A (Virogen, Watertown, MA, USA), or beta-actin (Sigma), and detected by a chemiluminescence reaction (BM Chemiluminescence Blotting Substrate; POD, Roche).

Transient-replication assays

A replicon, pRep-Fluc, was transfected into cells and the luciferase activities of the cell lysates were measured serially. To correct the transfection efficiency, each value was divided by the luciferase activity at 4 h after the transfection.

Stable colony formation assays

Cells were transfected with a replicon, pRep-BSD, and were cultured in the presence of 150 μg/mL of BSD (Invitrogen). BSD-resistant cell colonies appeared after ~3 weeks of culture, and were counted.

HCV-JFH1 virus cell culture

An *in-vitro* transcribed HCV-JFH1 RNA[26] was transfected into Huh7.5.1 cells.[27] Naive Huh7.5.1 cells were subsequently infected by the culture supernatant of the JFH1-RNA transfected Huh-7.5.1 cells, and subjected to siRNA or drug treatments. Replication levels of HCV-RNA were quantified by the realtime RT-PCR by using primers that targeted HCV-NS5B region, HCV-JFH1 sense: 5′-TCA GAC AGA GCC TGA GTC CA-3′, and HCV-JFH1 antisense: 5′-AGT TGC TGG AGG GCT TCT GA-3′.

Mice and adenovirus infection

Transgenic mice, CN2-29, inducibly express mRNA for the HCV structural proteins (genotype1b, nucleotides 294–3435) by the Cre/*lox*P switching system.[28] The transgene does not contain full-length HCV 5′-UTR, but shares the target sequence of the shRNA-HCV. Although the transgenic mouse CN2 has been previously reported as expressing higher levels of the viral proteins, the expression levels of the viral core protein in the CN2-29 mice are modest and similar to that in the liver of HCV patients. Thus, we chose CN2-29 mice in the present study.

The mice were infected with AxshRNA-HCV or controls (AxshRNA-Control or AxCAw1) in combination with AxCAN-Cre, which expressed Cre recombinase. Three days after the infection, the mice were killed and HCV core protein in the liver was measured as described below. The BALB/c mice were maintained in the Animal Care Facility of Tokyo Medial and Dental University, and transgenic mice were in the Tokyo Metropolitan Institute of Medical Science. Animal care was in accordance with institutional guidelines. The review board of the university approved our experimental animal studies and all experiments were approved by the institutional animal study committees.

Measurement of HCV core protein in mouse liver

The amounts of HCV core protein in the liver tissue from the mice was measured by a fluorescence enzyme immunoassay (FEIA)[29] with a slight modification. Briefly, the 5F11 monoclonal anti-HCV-core antibody was used as the first antibody on the solid phase, and the 5E3 antibody conjugated with horseradish peroxidase was the second antibody. This FEIA can detect as little as 4 pg/mL of recombinant HCV-core protein. Contents of the HCV core protein in the liver samples were normalized by the total protein contents and expressed as pg/mg total protein.

Immunohistochemical staining

Liver tissue was frozen with optimal cutting temperature (OTC) compound (Tissue Tek; Sakura Finetechnical, Tokyo, Japan). The sections (8 μm thick) were fixed with a 1:1 solution of acetone : methanol at −20°C for 10 min and then washed with phosphate-buffered saline (PBS). Subsequently, the sections were incubated with the IgG fraction of an anti-HCV core rabbit polyclonal antibody (RR8)[28] in blocking buffer or antialbumin rabbit polyclonal antibody (Dako Cytomation, Glostrup, Denmark) in PBS overnight at 4°C. The sections were incubated with secondary antibody, Alexa-antirabbit IgG (Invitrogen) or TRITIC-antirabbit IgG (Sigma), for 2 h at room temperature. Fluorescence was observed using a fluorescence microscope.

Statistical analyses

Statistical analyses were performed using Student's *t*-test; *P*-values of less than 0.05 were considered to be statistically significant.

Results

Retrovirus transduction of shRNA can protect from HCV replication

Retrovirus vectors propagated from pLNCshRNA-HCV and pLNCshRNA-Control were used to infect Huh7 cells, and cell lines were established that constitutively express shRNA-HCV and shRNA-Control (Huh7/shRNA-HCV and Huh7/shRNA-Control, respectively). There were no differences in the cell morphology or growth rate between shRNA-transduced and non-transduced Huh7 cells (data not shown). The HCV replicon, pRep-Fluc, was transfected into Huh7/shRNA-HCV, Huh7/shRNA-Control and naive Huh7 cells by electroporation. In Huh7/shRNA-Control and naive Huh7 cells, the initial luciferase activity at 4 h decreased temporarily, which represents decay of the transfected replicon RNA, but increased again at 48 h and 72 h, which demonstrate de novo synthesis of the HCV replicon RNA. In contrast, transfection into Huh7/shRNA-HCV cells resulted in a decrease in the initial luciferase activity, reaching background by 72 h (Fig. 3a). Similarly, transfection of the replicon, pRep-BSD, into Huh7 cells and BSD selection yielded numerous BSD-resistant colonies in the naive Huh7 (832 colonies) and Huh7/shRNA-Control cell lines (740 colonies), while transfection of Huh7/shRNA-HCV, which expressed shRNA-HCV, yielded obviously fewer colonies (five colonies), indicating reduction of colony forming units by $\sim 10^2$ (Fig. 3b). There was no difference in shape, growth or viability between cells expressing the shRNA or not. These results indicated that cells expressing HCV-directed shRNA following retrovirus transduction acquired resistance to HCV replication.

Effect of recombinant adenoviruses expressing shRNA on *in vitro* HCV replication

We investigated subsequently the effects of recombinant adenovirus vectors expressing shRNA. AxshRNA-HCV and AxshRNA-Control were used separately to infect Huh7/pRep-Feo cells, and the internal luciferase activities were measured sequentially (Fig. 4a). AxshRNA-HCV caused continuous suppression of HCV RNA replication. Six days postinfection, the luciferase activities fell to background levels. In contrast, the luciferase activities of the Huh7/pRep-Feo cells infected with AxshRNA-Control did not show any significant changes compared with untreated Huh7/pRep-Feo cells (Fig. 4a). The dimethylthiazol carboxymethoxyphenyl sulfophenyl tetrazolium (MTS) assay showed no significant difference between cells that were infected by recombinant adenovirus and uninfected cells (Fig. 4b). In the northern blotting analysis, the cells were harvested 6 days after infection with the adenovirus at an MOI of 1. Feo-replicon RNA of 9.6 kb, which was detectable in the untreated Huh7/pRep-Feo cells and in the cells infected with AxshRNA-Control, diminished substantially following infection with the AxshRNA-HCV (Fig. 4c). Densitometries showed that the intracellular levels of the replicon RNA in the Huh7/pRep-Feo cells correlated well with the internal luciferase activities. Similarly in the western blotting, cells were harvested 6 days after infection with adenovirus. Levels of the HCV NS4A and NS5A proteins that were translated from the HCV replicon decreased following infection with the AxshRNA-HCV

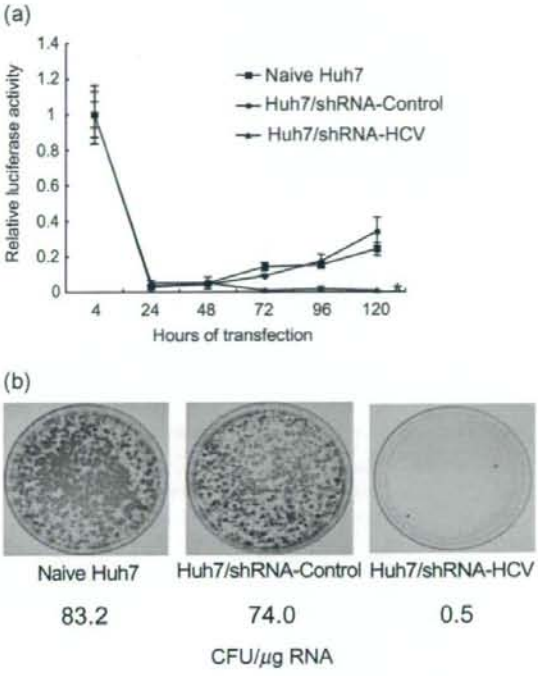

Figure 3 HCV replication can be inhibited by shRNA-HCV which was stably transfected into cells. Huh7/shRNA-HCV and Huh7/shRNA-Control stably express shRNA-HCV or shRNA-Control, respectively, following retroviral transduction. (a) Transient replication assay. An HCV replicon RNA, pRep-Fluc, was transfected into naive Huh7, Huh7/shRNA-HCV and Huh7/shRNA-Control cells. Luciferase activities of the cell lysates were measured serially at the times indicated, and the values were plotted as ratios relative to luciferase activities at 4 h. The luciferase activities at 4 h represent transfected replicon RNA. The data are mean ± SD. An asterisk denotes a *P*-value of less than 0.001 compared with the corresponding value of the naive Huh7 cells. (b) Stable colony formation assay. The HCV replicon, pRep-BSD, was transfected into naive Huh7, Huh7/shRNA-HCV and Huh7/shRNA-Control cells. The cells were cultured in the presence of blasticidin S (BSD) in the medium for ~3 weeks, and the BSD-resistant colonies were counted. These assays were repeated twice. The colony-forming units per microgram RNA (CFU/μg RNA) are shown at the bottom.

(Fig. 4d). These results indicated that the decrease in luciferase activities was due to specific suppressive effects of shRNA on expression of HCV genomic RNA and the viral proteins, and not due to non-specific effects caused by the delivery of shRNA or to toxicity of the adenovirus vectors.

Absence of interferon-stimulated gene responses by siRNA delivery

It has been reported that double-stranded RNA may induce interferon-stimulated gene (ISG) responses which cause instability of mRNA, translational suppression of proteins and apoptotic cell

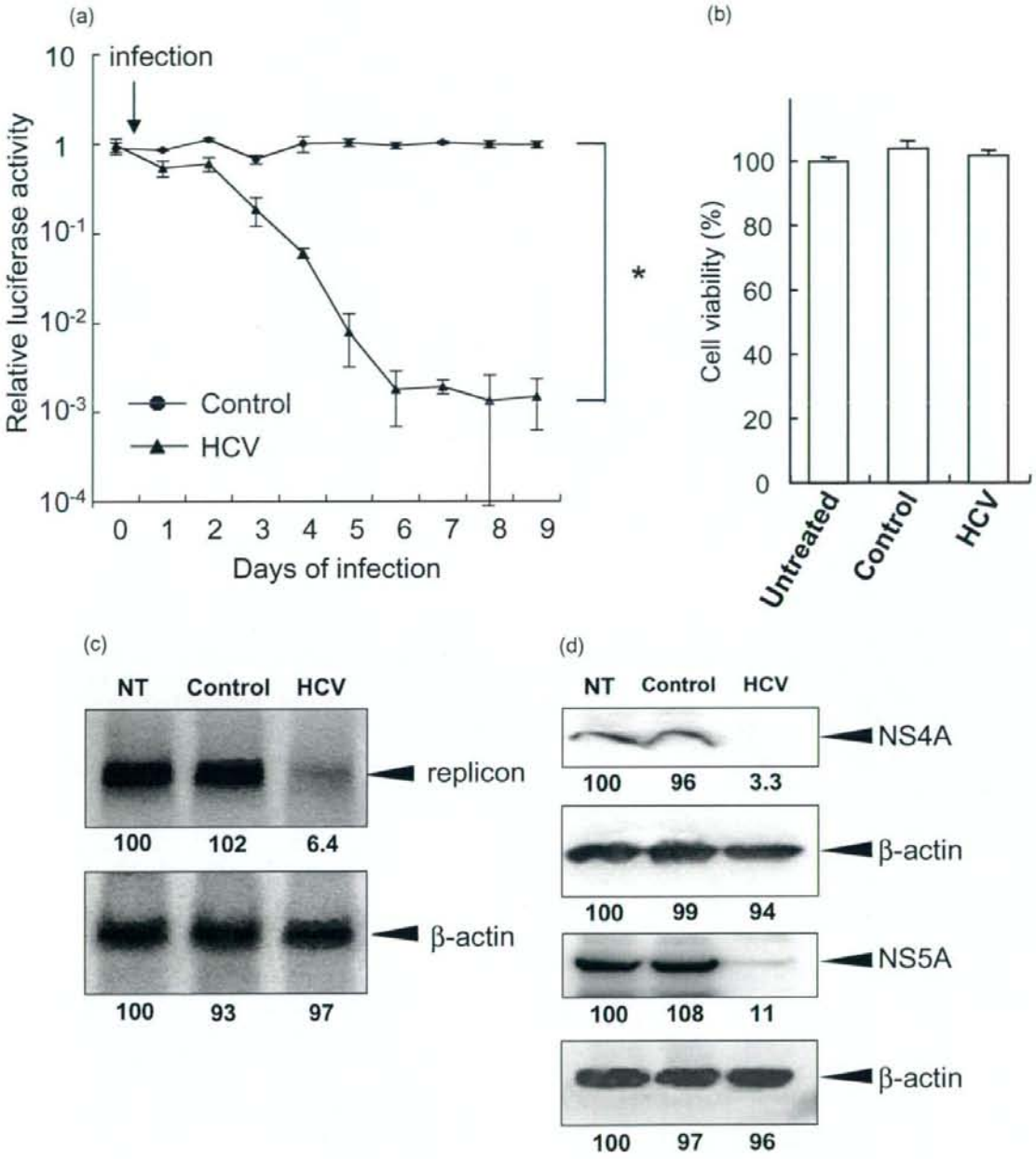

death.[18,30,31] Therefore, we examined the effects of the shRNA-expressing plasmids and adenoviruses on the activation of ISG expression in cells. The ISRE-reporter plasmid, pISRE-TA-Luc, and a control plasmid, peGFPneo, were transfected into Huh7 cells with plasmid pUC19-shRNA-HCV or pUC19-shRNA-Control, or adenovirus, AxshRNA-HCV or AxshRNA-Control, and the ISRE-mediated luciferase activities were measured. On day 2, the ISRE-luciferase activities did not significantly change in cells in which

Journal of Gastroenterology and Hepatology **23** (2008) 1437–1447

Figure 4 Effect of a recombinant adenovirus expressing shRNA on HCV replicon. (a) Huh7/pRep-Feo cells were infected with AxshRNA-HCV or shRNA-Control at a multiplicity of infection (MOI) of 1. The cells were harvested, and internal luciferase activities were measured on day 0 though day 9 after adenovirus infection. Each assay was done in triplicate, and the value is displayed as a percentage of no treatment and as mean ± SD. An asterisk indicates a *P*-value of less than 0.05. (b) Dimethylthiazol carboxymethoxyphenyl sulfophenyl tetrazolium (MTS) assay of Huh7/pRep-Feo cells. Cells were infected with indicated recombinant adenoviruses at an MOI of 1. The assay was done at day 6 of infection. Error bars indicate mean + SD. (c) Northern blotting. The upper panel shows replicon RNA, and the lower panel shows beta-actin mRNA. (d) Western blotting. Total cell lysates were separated on NuPAGE gel, blotted and incubated with monoclonal anti-NS4A or anti-NS5A antibodies. The membrane was re-blotted with antibeta-actin antibodies. NT, untreated Huh7/pRep-Feo cells; Control, cells infected with AxshRNA-Control; HCV, cells treated with AxshRNA-HCV. In panels (b) and (c), cells were harvested on day 6 after adenovirus infection at an MOI of 1.

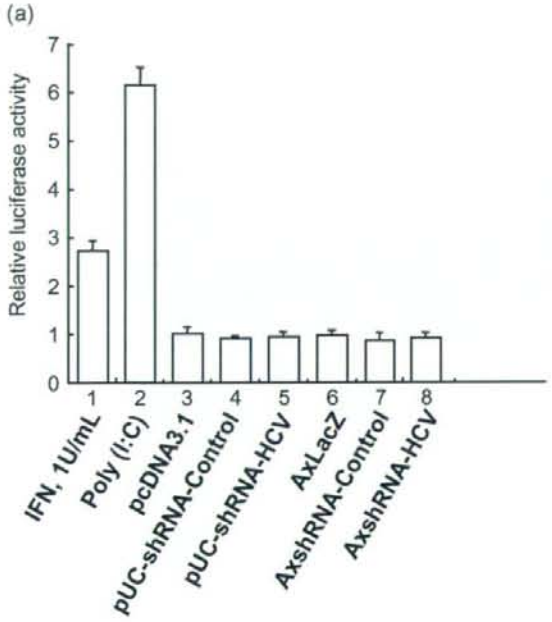

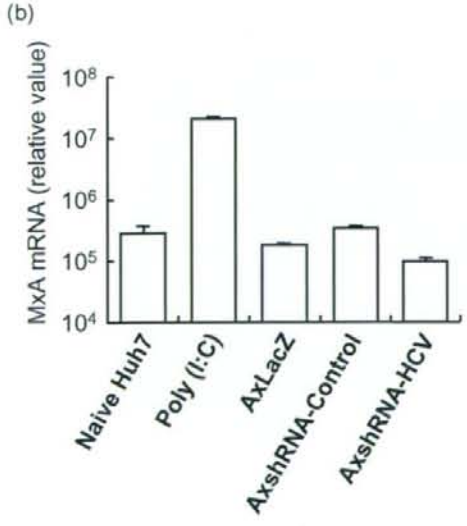

Figure 5 Interferon-stimulated gene responses by transfection of siRNA vectors. (a) Huh7 cells were seeded at 5×10^4 per well in 24-well plates on the day before transfection. As a positive control, 200 ng of pISRE-TA-Luc, or pTA-Luc, 1 ng of pRL-CMV, were transfected into a well using FuGENE-6 Transfection Reagent (Roche), and the cells were cultured with 1 U/mL of interferon (IFN) in the medium (lane 1). Lanes 3–5: 200 ng of pISRE-TA-Luc or pTA-Luc, and 1 ng of pRL-CMV were cotransfected with (lane2) 300 ng of poly (I : C), or 200 ng of plasmids (lane 3) pcDNA3.1, (lane 4) pUC19-shRNA-Control or (lane 5) pUC19-shRNA-HCV. Lanes 6–8: 200 ng of pISRE-TA-Luc or pTA-Luc, and 1 ng of pRL-CMV were transfected, and MOI = 1 of adenoviruses, (lane 6) AxLacZ, which expressed the beta-galactosidase (LacZ) gene under control of the chicken beta-actin (CAG) promoter as a control, (lane 7) AxshRNA-Control or (lane 8) AxshRNA-HCV were infected. Dual luciferase assays were performed at 48 h after transfection. The Fluc activity of each sample was normalized by the respective Rluc activity, and the respective pTA luciferase activity was subtracted from the pISRE luciferase activity. The experiment was done in triplicate, and the data are displayed as means + SD. (b) Huh7 cells were infected with indicated recombinant adenoviruses, AxLacZ, AxshRNA-Control and AxshRNA-HCV. RNA was extracted from each sample at day 6, and mRNA expression levels of an interferon-inducible MxA protein were quantified by the real-time RT-PCR analysis. Primers used were as follows: human MxA sense, 5′-CGA GGG AGA CAG GAC CAT CG-3′; human MxA antisense, 5′-TCT ATC AGG AAG AAC ATT TT-3′; human beta-actin sense, 5′-ACA ATG AAG ATC AAG ATC ATT GCT CCT CCT-3′; and human beta-actin antisense, 5′-TTT GCG GTG GAC GAT GGA GGG GCC GGA CTC-3′.

negative- or positive-control shRNA plasmids was transfected. (Fig. 5a). Similarly, the expression levels of an interferon-inducible MxA protein did not significantly change by transfection of shRNA-expression vectors (Fig. 5b). These results demonstrate that the shRNA used in the present study lack induction of the ISG responses both in the form of the expression plasmids and the adenovirus vectors.

Effect of siRNA and shRNA adenoviruses on HCV-JFH1 cell culture

The effects of HCV-targeted siRNA- and shRNA-expressing adenoviruses were confirmed by using HCV-JFH1 virus cell culture system. Transfection of the siRNA #331[14] into HCV-infected Huh7.5.1 cells resulted in substantial decrease of intracellular HCV RNA, while a control siRNA showed no effect (Fig. 6a). Similarly, infection of AxshRNA-HCV into Huh7.5.1/HCV-JFH1 cells specifically suppressed expression of HCV RNA (Fig. 6b).

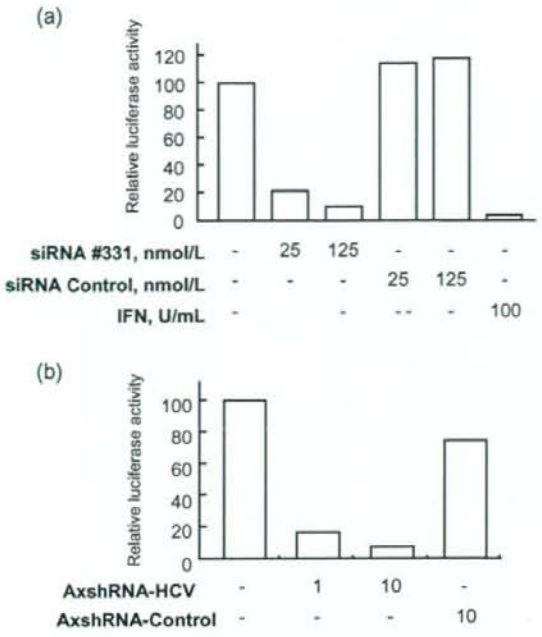

Figure 6 Effects of an siRNA and adenovirus expressing shRNA on HCV-JFH1 cell culture. (a) The siRNA #331, the siRNA-Control[14], (b) AxshRNA-HCV or AxshRNA-Control were, respectively, transfected or infected onto HV-JFH1-infected Huh7.5.1 cells. Seventy-two hours of the transfection or infection, expression level of HCV-RNA was quantified by real-time RT-PCR. The assays were repeated twice, and consistent results were obtained. IFN, recombinant interferon-alpha 2b.

Suppression of HCV-IRES-mediated translation *in vivo* by adenovirus expressing shRNA

The effects of the shRNA expression on the expression of the viral structural proteins *in vivo* were investigated using conditional HCV cDNA-transgenic mice, CN2-29.[28] Adenoviruses, AxshRNA-HCV, AxshRNA-Control or AxCAw1 were injected into CN2-29 mice in combination with AxCANCre, an adenovirus expressing *Cre* DNA recombinase. The mice were killed on the fourth day after the injection, and the hepatic expression of the HCV core protein was measured. The expressed amounts of the core protein were 143.0 ± 56.2 pg/mg and 108.5 ± 42.4 pg/mg in AxCAw1 and AxshRNA-Control-infected mice, respectively, and the expressed amount was significantly lower in mice injected with AxshRNA-HCV (28.7 ± 7.0 pg/mg, $P < 0.05$, Fig. 7a). Similarly, the induced expression of HCV core protein was not detectable by immunohistochemistry in AxshRNA-HCV infected liver tissue (Fig. 7c). Staining of a host cellular protein, albumin, was not obviously different between the liver infected with AxCAw1, AxshRNA-HCV and AxshRNA-Control (Fig. 7d). The expression levels of two ISG, IFN-beta and Mx1, in the liver tissue were not significantly different between individuals with and without injection of the adenovirus vectors (Fig. 7b). These results indicate specific shRNA silencing of HCV structural protein expression in the liver.

Discussion

The requirements to achieve a high efficiency using RNAi are: (i) selection of target sequences that are the most susceptible to RNAi; (ii) persistence of siRNA activity; and (iii) efficient *in vivo* delivery of siRNA to cells. We have used an shRNA sequence that was derived from a highly efficient siRNA (siRNA331), and constructed a DNA-based shRNA expression cassette that showed competitive effects with the synthetic siRNA (Fig. 2).[14] The shRNA-expression cassette does not only allow extended half-life of the RNAi, but also enables use of gene-delivery vectors, such as virus vectors. As shown in the results, a retrovirus vector expressing shRNA-HCV could stably transduce cells to express HCV-directed shRNA, and the cells acquired protection against HCV subgenomic replication (Fig. 3). An adenovirus vector expressing shRNA-HCV resulted in suppression of HCV subgenomic and protein expression by around three logs to almost background levels (Fig. 4). Consistent results were obtained by using an HCV cell culture (Fig. 6). More importantly, we have demonstrated *in-vivo* effects on viral protein expression in the liver using a conditional transgenic mouse model (Fig. 7). These results suggest that efficient delivery of siRNA could be effective against HCV infection *in vivo*.

An obstacle to applying siRNA technology to treat virus infections is that viruses are prone to mutate during their replication.[32] HCV continuously produces mutated viral strains to escape immune defense mechanisms. Even in a single patient, the circulating HCV population comprises a large number of closely related HCV sequence variants called quasispecies. Therefore, siRNA targeting the protein-coding sequence of the HCV genome, which have been reported by others,[15–19] may vary considerably among different HCV genotypes, and even among strains of the same genotype.[33] Our shRNA sequence targeted the 5′-UTR of HCV RNA, which is the most conserved region among various HCV isolates.[33] In addition, the structural constraints on the 5′-UTR, in terms of its requirement to direct internal ribosome entry and translation of viral proteins, might not permit the evolution of escape mutations. Our preliminary results have shown that the siRNA-HCV suppressed replication of an HCV genotype 2a replicon[34] to the same extent as the HCV 1b replicon.

Although the siRNA techniques rely on a high degree of specificity, several studies report siRNA-induced non-specific effect that may result from induction of ISG responses.[18,31] These effects may be mediated by activation of double-strand RNA-dependent protein kinase, toll-like receptor 3,[35] or possibly by a recently identified RNA helicase, RIG-I.[36] It remains to be determined whether these effects are generally induced by every siRNA construct. Sledz *et al.* have reported that transfection of two siRNA induced cellular interferon responses,[37] while Bridge *et al.* report that shRNA-expressing plasmids induced an interferon response but transfection of synthetic siRNA did not.[31] Speculatively, these effects on the interferon system might be construct dependent. Our shRNA-expression plasmids and adenoviruses did not activate ISG responses *in vitro* (Fig. 5a,b) or *in vivo* (Fig. 7b). We have preliminarily detected phosphorylated PKR (P-PKR) by western

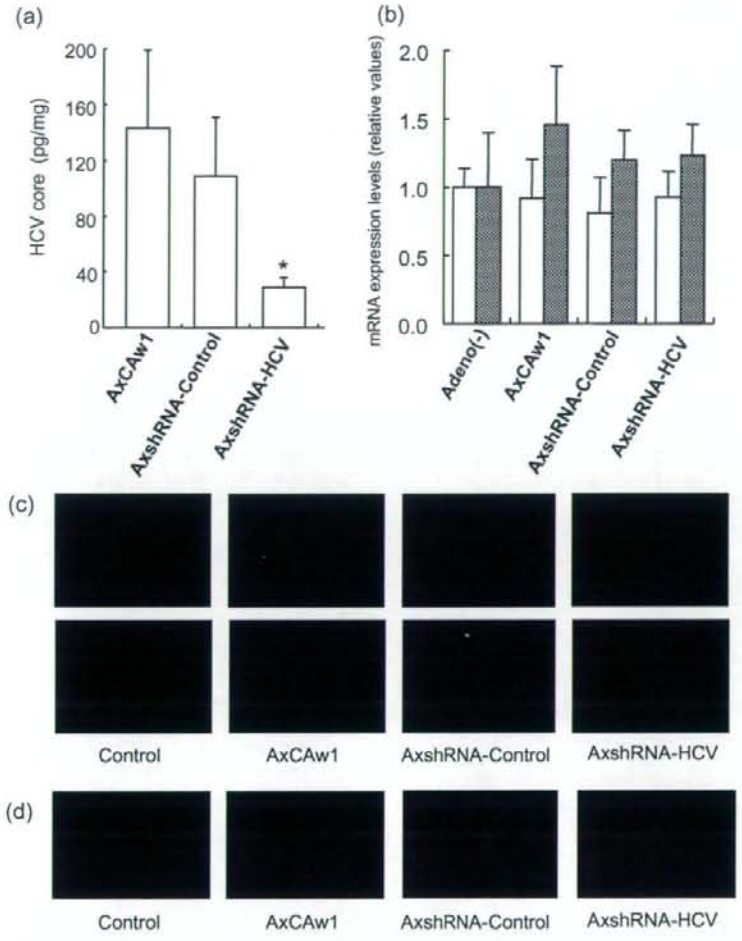

Figure 7 Effects of a recombinant adenovirus expressing shRNA on HCV core protein expression in CN2-29 transgenic mice. CN2-29 transgenic mice were administered with 1×10^9 PFU of AxCANCre combined with 6.7×10^8 PFU of AxshRNA-HCV, AxshRNA or AxCAw1. The mice were killed on day 4 after injection. (a) Quantification of HCV core protein in liver. Liver tissues were homogenized and used to determine the amount of HCV core protein. Each assay was done in triplicate, and the values are displayed as mean ± SD. Asterisk indicates *P*-value of less than 0.05. (b) Expression levels of mouse interferon-beta (white bars) and Mx1 (shaded bars) mRNA in the mouse liver tissue were quantified by the real-time RT-PCR analyses. Primers used were as follows: mouse interferon-beta sense, 5′-ACA GCC CTC TCC ATC AAC TA-3′; mouse interferon-beta antisense, 5′-CCC TCC AGT AAT AGC TCT TC-3′; mouse Mx1 sense, 5′-AGG AGT GGA GAG GCA AAG TC-3′; mouse Mx1 antisense, 5′-CAC ATT GCT GGG GAC TAC CA-3′; mouse beta-actin sense, 5′-ACT CCT ATG TGG GTG ACG AG-3′; mouse beta-actin antisense, 5′-ATA GCC CTC GTA GAT GGG CA-3′. Adeno (-) denotes mice without adenovirus administration. (c) Immunofluorescence microscopy of HCV core protein in the liver tissue. Liver sections of mice were stained using rabbit anticore polyclonal antibody and normal rabbit IgG as a negative control. The upper photographs were obtained at 400× magnification, and the lower photographs were at 1000×. (d) Immunofluorescence microscopy of albumin in liver. Liver sections from the mice were fixed and stained using rabbit antialbumin antibody and normal rabbit IgG as a negative control.

blotting, and found no apparent increase of P-PKR (data not shown). These results indicate that these target sequences and structures are of sufficient specificity to silence the target gene without eliciting non-specific interferon responses.

Beside the canonical action of siRNA, a sequence-specific cleavage of target mRNA, the siRNA could act as a micro-RNA that suppresses translational initiation of mRNA,[38] or it could mediate transcriptional gene silencing.[39] Regarding our *in-vivo* experiments, it was difficult to differentially analyze the effect of siRNA at individual sites of action because post-translational effect of siRNA concomitantly destabilizes target mRNA, which leads to apparent decrease of mRNA transcripts.

Efficiency and safety of gene transfer methods are the key determinants of the clinical success of gene therapy and an unresolved problem. There are several reports of delivery of siRNA or siRNA-expression vectors to cells *in vivo*;[12,40,41] however, gene delivery methods that are safe enough to apply to clinical therapeutics are currently under development. Adenovirus vectors are one of the most commonly used carriers for human gene therapies.[42–44] Our present results demonstrate that the adenoviral delivery of shRNA is effective in blocking HCV replication *in vitro* and virus protein expression *in vivo*. Adenovirus vectors have several advantages of efficient delivery of transgene both *in vitro* and *in vivo* and natural hepatotropism when administered *in vivo*. The AxshRNA-HCV specifically blocked expression of HCV structural proteins in a conditional transgenic mouse expressing those proteins. The current adenovirus vectors may cause inflammatory reactions in the target organ,[45] however, and produce neutralizing antibodies which make repeated administration difficult. These problems may be overcome by the improved constructs of virus vectors with attenuated immunogenicity or by the development of non-viral carriers for gene delivery.[46]

In conclusion, our results demonstrate the effectiveness and feasibility of the siRNA expression system. The efficiency of adenovirus expressing shRNA that target HCV suggests that delivery and expression of siRNA in hepatocytes may eliminate the virus and that this RNA-targeting approach might provide a potentially effective future therapeutic option for HCV infection.

Acknowledgments

This study was supported by grants from Japan Society for the Promotion of Science, 15590629 and 16590580, and partly supported by a grant from the Viral Hepatitis Research Foundation of Japan.

References

1 Alter MJ. Epidemiology of hepatitis C. *Hepatology* 1997; **26**: 62S–65S.
2 Hadziyannis SJ, Sette H Jr, Morgan TR *et al.* Peginterferon-alpha2a and ribavirin combination therapy in chronic hepatitis C: a randomized study of treatment duration and ribavirin dose. *Ann. Intern. Med.* 2004; **140**: 346–55.
3 Fire A, Xu S, Montgomery M, Kostas S, Driver S, Mello C. Potent and specific genetic interference by double-stranded RNA in Caenorhabditis elegans. *Nature* 1998; **19**: 806–11.
4 Elbashir SM, Harborth J, Lendeckel W, Yalcin A, Weber K, Tuschl T. Duplexes of 21-nucleotide RNAs mediate RNA interference in cultured mammalian cells. *Nature* 2001; **411**: 494–8.
5 Coburn GA, Cullen BR. Potent and specific inhibition of human immunodeficiency virus type 1 replication by RNA interference. *J. Virol.* 2002; **76**: 9225–31.
6 Jacque JM, Triques K, Stevenson M. Modulation of HIV-1 replication by RNA interference. *Nature* 2002; **418**: 435–8.
7 Gitlin L, Karelsky S, Andino R. Short interfering RNA confers intracellular antiviral immunity in human cells. *Nature* 2002; **418**: 430–4.
8 Ge Q, Filip L, Bai A, Nguyen T, Eisen HN, Chen J. Inhibition of influenza virus production in virus-infected mice by RNA interference. *Proc. Natl. Acad. Sci. USA* 2004; **101**: 8676–81.
9 Wang C, Pflugheber J, Sumpter R Jr *et al.* Alpha interferon induces distinct translational control programs to suppress hepatitis C virus RNA replication. *J. Virol.* 2003; **77**: 3898–912.
10 Klein C, Bock CT, Wedemeyer H *et al.* Inhibition of hepatitis B virus replication in vivo by nucleoside analogues and siRNA. *Gastroenterology* 2003; **125**: 9–18.
11 Konishi M, Wu CH, Wu GY. Inhibition of HBV replication by siRNA in a stable HBV-producing cell line. *Hepatology* 2003; **38**: 842–50.
12 McCaffrey AP, Meuse L, Pham TT, Conklin DS, Hannon GJ, Kay MA. RNA interference in adult mice. *Nature* 2002; **418**: 38–9.
13 Shlomai A, Shaul Y. Inhibition of hepatitis B virus expression and replication by RNA interference. *Hepatology* 2003; **37**: 764–70.
14 Yokota T, Sakamoto N, Enomoto N *et al.* Inhibition of intracellular hepatitis C virus replication by synthetic and vector-derived small interfering RNAs. *EMBO Rep.* 2003; **4**: 602–8.
15 Kapadia SB, Brideau-Andersen A, Chisari FV. Interference of hepatitis C virus RNA replication by short interfering RNAs. *Proc. Natl. Acad. Sci. USA* 2003; **100**: 2014–18.
16 Kronke J, Kittler R, Buchholz F *et al.* Alternative approaches for efficient inhibition of hepatitis C virus RNA replication by small interfering RNAs. *J. Virol.* 2004; **78**: 3436–46.
17 Randall G, Grakoui A, Rice CM. Clearance of replicating hepatitis C virus replicon RNAs in cell culture by small interfering RNAs. *Proc. Natl. Acad. Sci. USA* 2003; **100**: 235–40.
18 Seo MY, Abrignani S, Houghton M, Han JH. Letter to the editor: small interfering RNA-mediated inhibition of hepatitis C virus replication in the human hepatoma cell line Huh-7. *J. Virol.* 2003; **77**: 810–12.
19 Wilson JA, Jayasena S, Khvorova A *et al.* RNA interference blocks gene expression and RNA synthesis from hepatitis C replicons propagated in human liver cells. *Proc. Natl. Acad. Sci. USA* 2003; **100**: 2783–8.
20 Guo JT, Bichko VV, Seeger C. Effect of alpha interferon on the hepatitis C virus replicon. *J. Virol.* 2001; **75**: 8516–23.
21 Tanabe Y, Sakamoto N, Enomoto N *et al.* Synergistic inhibition of intracellular hepatitis C virus replication by combination of ribavirin and interferon-alpha. *J. Infect. Dis.* 2004; **189**: 1129–39.
22 Maekawa S, Enomoto N, Sakamoto N *et al.* Introduction of NS5A mutations enables subgenomic HCV-replicon derived from chimpanzee-infectious HC-J4 isolate to replicate efficiently in Huh-7 cells. *J. Viral. Hepat.* 2004; **11**: 394–403.
23 Miyagishi M, Sumimoto H, Miyoshi H, Kawakami Y, Taira K. Optimization of an siRNA-expression system with an improved hairpin and its significant suppressive effects in mammalian cells. *J. Gene Med.* 2004; **6**: 715–23.
24 Li Y, Yokota T, Matsumura R, Taira K, Mizusawa H. Sequence-dependent and independent inhibition specific for mutant ataxin-3 by small interfering RNA. *Ann. Neurol.* 2004; **56**: 124–9.
25 Kanazawa N, Kurosaki M, Sakamoto N *et al.* Regulation of hepatitis C virus replication by interferon regulatory factor-1. *J. Virol.* 2004; **78**: 9713–20.
26 Wakita T, Pietschmann T, Kato T *et al.* Production of infectious hepatitis C virus in tissue culture from a cloned viral genome. *Nat. Med.* 2005; **11**: 791–6.
27 Zhong J, Gastaminza P, Cheng G *et al.* Robust hepatitis C virus infection in vitro. *Proc. Natl. Acad. Sci. USA* 2005; **102**: 9294–9.
28 Wakita T, Taya C, Katsume A *et al.* Efficient conditional transgene expression in hepatitis C virus cDNA transgenic mice mediated by the Cre/loxP system. *J. Biol. Chem.* 1998; **273**: 9001–6.
29 Kashiwakuma T, Hasegawa A, Kajita T *et al.* Detection of hepatitis C virus specific core protein in serum of patients by a sensitive fluorescence enzyme immunoassay (FEIA). *J. Immunol. Methods* 1996; **28**: 79–89.

30 Baglioni C, Nilsen TW. Mechanisms of antiviral action of interferon. *Interferon* 1983; **5**: 23–42.
31 Bridge A, Pebernard S, Ducraux A, Nicoulaz A, Iggo R. Induction of an interferon response by RNAi vectors in mammalian cells. *Nat. Genet.* 2003; **34**: 263–4.
32 Carmichael GG. Silencing viruses with RNA. *Nature* 2002; **418**: 379–80.
33 Okamoto H, Okada S, Sugiyama Y *et al.* Nucleotide sequence of the genomic RNA of hepatitis C virus isolated from a human carrier: comparison with reported isolates for conserved and divergent regions. *J. Gen. Virol.* 1991; **72**: 2697–704.
34 Kato T, Date T, Miyamoto M *et al.* Efficient replication of the genotype 2a hepatitis C virus subgenomic replicon. *Gastroenterology* 2003; **125**: 1808–17.
35 Alexopoulou L, Holt AC, Medzhitov R, Flavell RA. Recognition of double-stranded RNA and activation of NF-kB by Toll-like receptor 3. *Nature* 2001; **413**: 732–8.
36 Yoneyama M, Kikuchi M, Natsukawa T *et al.* The RNA helicase RIG-I has an essential function in double-stranded RNA-induced innate antiviral responses. *Nat. Immunol.* 2004; **5**: 730–7.
37 Sledz C, Holko M, de Veer M, Silverman R, Williams, B. Activation of the interferon system by short-interfering RNAs. *Nat. Cell. Biol.* 2003; **5**: 834–9.
38 Doench JG, Petersen CP, Sharp PA. siRNAs can function as miRNAs. *Genes Dev.* 2003; **17**: 438–42.
39 Morris KV. siRNA-mediated transcriptional gene silencing: the potential mechanism and a possible role in the histone code. *Cell. Mol. Life Sci.* 2005; **62**: 3057–66.
40 Xia H, Mao Q, Paulson HL, Davidson BL. siRNA-mediated gene silencing in vitro and in vivo. *Nat. Biotechnol.* 2002; **20**: 1006–10.
41 Zender L, Hutker S, Liedtke C *et al.* Caspase 8 small interfering RNA prevents acute liver failure in mice. *Proc. Natl. Acad. Sci. USA* 2003; **100**: 7797–802.
42 Akli S, Caillaud C, Vigne E *et al.* Transfer of a foreign gene into the brain using adenovirus vectors. *Nat. Genet.* 1993; **3**: 224–8.
43 Bajocchi G, Feldman SH, Crystal RG, Mastrangeli A. Direct in vivo gene transfer to ependymal cells in the central nervous system using recombinant adenovirus vectors. *Nat. Genet.* 1993; **3**: 229–34.
44 Davidson BL, Allen ED, Kozarsky KF, Wilson JM, Roessler BJ. A model system for in vivo gene transfer into the central nervous system using an adenoviral vector. *Nat. Genet.* 1993; **3**: 219–23.
45 Yang Y, Wilson JM. Clearance of adenovirus-infected hepatocytes by MHC class I-restricted CD4+ CTLs in vivo. *J. Immunol.* 1995; **155**: 2564–70.
46 Fleury S, Driscoll R, Simeoni E *et al.* Helper-dependent adenovirus vectors devoid of all viral genes cause less myocardial inflammation compared with first-generation adenovirus vectors. *Basic Res. Cardiol.* 2004; **99**: 247–56.

Bioorganic & Medicinal Chemistry xxx (2009) xxx–xxx

Contents lists available at ScienceDirect

Bioorganic & Medicinal Chemistry

journal homepage: www.elsevier.com/locate/bmc

Synthesis of nuclease-resistant siRNAs possessing universal overhangs

Yoshihito Ueno [a,b,c,f,*], Yuuji Watanabe [a], Aya Shibata [a], Kayo Yoshikawa [a], Takashi Takano [e], Michinori Kohara [e], Yukio Kitade [a,b,c,d,*]

[a] Department of Biomolecular Science, Faculty of Engineering, Gifu University, 1-1 Yanagido, Gifu 501-1193, Japan
[b] United Graduate School of Drug Discovery and Medical Information Sciences, Gifu University, 1-1 Yanagido, Gifu 501-1193, Japan
[c] Center for Emerging Infectious Diseases, Gifu University, 1-1 Yanagido, Gifu 501-1193, Japan
[d] Center for Advanced Drug Research, Gifu University, 1-1 Yanagido, Gifu 501-1193, Japan
[e] Department of Microbiology and Cell Biology, The Tokyo Metropolitan Institute of Medical Science, 3-18-22, Honkomagome, Bunkyo-ku, Tokyo 113-8613, Japan
[f] PRESTO, JST (Japan Science and Technology Agency), 4-1-8 Honcho Kawaguchi, Saitama 332-0012, Japan

ARTICLE INFO

Article history:
Received 28 November 2008
Revised 14 January 2009
Accepted 15 January 2009
Available online xxxx

Keywords:
RNAi
siRNA
Aromatic compound
Nuclease-resistant
HCV

ABSTRACT

RNA interference (RNAi) induced by small interfering RNA (siRNA) has emerged as a powerful technique for the silencing of gene expression at the post-transcriptional level. It has been shown that in the RNAi machinery, the 3′-overhang region of a guide strand (an antisense strand) of siRNA is recognized by the PAZ domain in the Argonaute protein, and the 2-nucleotide (nt) 3′-overhang is accommodated into a binding pocket composed of hydrophobic amino acids in the PAZ domain. Based on this background information, we designed and synthesized siRNAs possessing aromatic compounds at their 3′-overhang regions. It was found that the modified siRNAs possessing aromatic compounds are more potent than the siRNAs without the 3′-overhang regions. Further, the silencing activities of the modified siRNAs are almost equal to those of normal siRNAs with natural nucleosides at their 3′-overhang regions. We also found that the siRNAs possessing the aromatic compounds at their 3′-overhang region could be used to inhibit hepatitis C virus (HCV) replication. Moreover, the RNAs with aromatic groups at their 3′-ends were more resistant to nucleolytic degradation by snake venom phosphodiesterase (SVPD) (a 3′-exonuclease) than natural RNAs. The aromatic compounds described in this report do not have functional groups capable of forming hydrogen bonds with nucleobases. Therefore, we expect that they can serve as the universal overhang units that can improve the nuclease resistance of siRNAs.

1. Introduction

RNA interference (RNAi) is a process of sequence-specific post-transcriptional gene silencing that is triggered by double-stranded RNAs (dsRNAs) homologous to the silenced genes.[1] The process is initiated by the processive cleavage of dsRNA into 21- to 23-nucleotide (nt) duplexes by the enzyme Dicer. These duplexes, which contain a 2-nt overhang at the 3′-end of each strand, are termed as short interfering RNAs (siRNAs). The siRNAs associate with the RNA-induced silencing complex (RISC), which is then guided to catalyze the sequence-specific degradation of the target mRNA.[2–4]

siRNA has considerable potential as a new therapeutic drug for intractable diseases because siRNAs can be rationally designed and synthesized if the sequences of the disease-causing genes are known. Several groups have demonstrated the efficacy of siRNA-mediated inhibition of clinically relevant genes in vivo as well as in vitro.[4–6] Improving the nuclease resistance of siRNA is important for the therapeutic application of synthetic siRNAs.[4] Thus far, many types of siRNAs modified at the base, sugar, or phosphate moieties have been synthesized, and their nuclease-resistant properties and RNAi-inducing activities have been studied.[7–26]

Argonaute2, a key component of RISC, is responsible for mRNA cleavage in the RNAi pathway.[27,28] Argonaute2 is composed of PAZ, Mid, and PIWI domains. X-ray structural analysis and a nuclear magnetic resonance (NMR) study have revealed that the 2-nt 3′-overhang region of the guide strand (the antisense strand) of siRNA is recognized by the PAZ domain and is accommodated into a binding pocket composed of hydrophobic amino acids; this pocket is located in the domain.[29–32] The length of the 3′-overhang regions of siRNA influences the activities of the siRNAs. It is reported that the 2-nt 3′-overhang is the most efficient in an experiment using 21-nt siRNA in *Drosophila* embryo lysate; however, the multiple addition of 2′-deoxynucleotide to the 3′-end of siRNAs is tolerated.[33]

Considering this background information, we substituted the natural nucleosides at 3′-overhang regions with the aromatic compounds, 1,3-bis(hydroxymethyl)benzene (**1**), 1,3-bis(hydroxymethyl)pyridine (**2**), and 1,2-bis(hydroxymethyl)benzene (**3**) (Fig. 1). We hypothesized that the introduction of lipophilic groups

* Corresponding authors. Tel.: +81 58 293 2639; fax: +81 58 293 2794 (Y.U.).
E-mail addresses: uenoy@gifu-u.ac.jp (Y. Ueno), ykkitade@gifu-u.ac.jp (Y. Kitade).

0968-0896/$ - see front matter © 2009 Elsevier Ltd. All rights reserved.
doi:10.1016/j.bmc.2009.01.033

Please cite this article in press as: Ueno, Y. et al., *Bioorg. Med. Chem.* (2009), doi:10.1016/j.bmc.2009.01.033

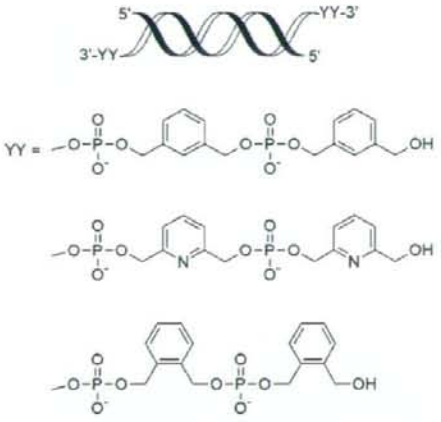

Figure 1. Structures of the siRNAs.

at the 3′-overhang portions of the siRNAs would improve affinities of the 3′-overhang portions of the siRNAs with the PAZ protein making the siRNAs more potent than normal siRNAs which possess natural nucleosides at their 3′-overhang portion. In addition, the modified RNAs would be more nuclease-resistant than the normal siRNAs.

In this paper, we report the synthesis and the silencing activities of the siRNAs with the aromatic groups **1–3** at their 3′-overhang regions. The nuclease-resistant properties of the siRNAs are also reported.

2. Results

2.1. Synthesis

Modified siRNAs were synthesized by the phophoramidite method. In order to incorporate the aromatic compounds at the 3′-overhang regions of siRNAs, solid supports carrying **1**, **2**, or **3** and phosphoramidites of **1**, **2**, and **3** were synthesized according to routes shown in Schemes 1 and 2. Dimethyl isophtalate was treated with $LiBH_4$ to give 1,3-bis(hydroxymethyl)benzene (**1**) in 95% yield. One of the two hydroxyl groups of **1** was protected with a 4,4′-dimethoxytrityl (DMTr) group to afford a mono-DMTr derivative **6** in 51% yield. The mono-DMTr derivative **6** was phosphitylated by the standard procedure[34] to produce the corresponding phosphoramidite **8** in 94% yield. In a similar manner, the phosphoramidites **9** and **14** were synthesized from dimethyl 2,6-pyridinedicarboxylate and dimethyl phthalate with total yields of 13% and 64%, respectively.

To enable attachment to the solid support, the mono-DMTr derivative **6** was succinated to yield the corresponding succinate, that was linked to controlled pore glass (CPG) to afford the solid support **10** possessing **6** (108 μmol/g). Similarly, the mono-DMTr derivatives **7** and **13** were succinated and then linked to the CPGs to afford the solid supports **11** and **15** possessing **7** (74 μmol/g) and **13** (86 μmol/g), respectively.

2.2. Oligoribonucleotide synthesis

All oligoribonucleotides (ONs) were synthesized with a DNA/RNA synthesizer. Fully protected ONs (1.0 μmol each) linked to solid supports were treated with concentrated NH_4OH:EtOH (3:1, v/v)

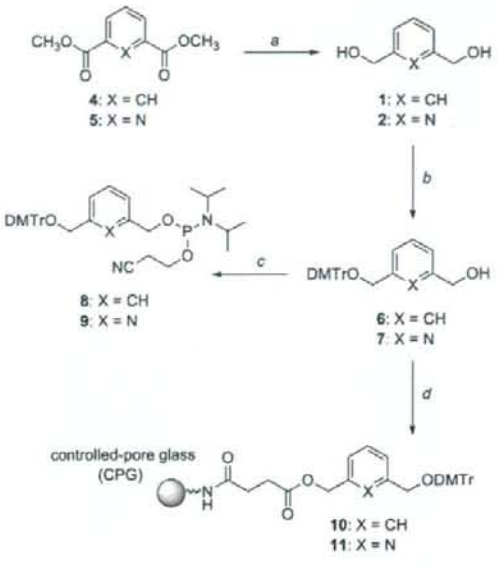

Scheme 1. Reagents and conditions: (a) $LiBH_4$, THF, rt, 95% for **1** and 28% for **2**; (b) DMTrCl, DMAP, pyridine, rt, 51% for **6** and 51% for **7**; (c) chloro(2-cyanoethoxy)(*N*,*N*-diisopropylamino)phosphine, *i*-Pr_2NEt, THF, rt, 94% for **8** and 93% for **9**; (d) (1) succinic anhydride, DMAP, pyridine, rt; (2) CPG, WSCl, DMF, rt, 108 μmol/g for **10** and 74 μmol/g for **11**.

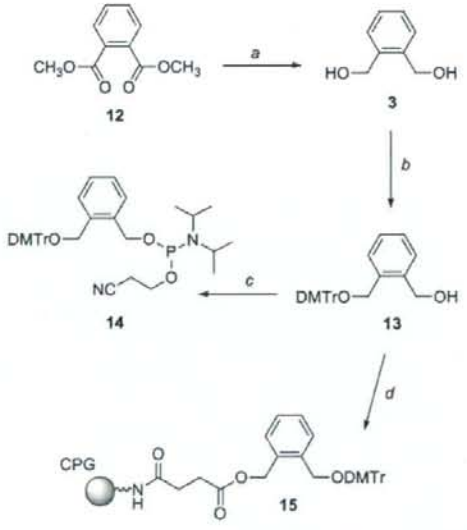

Scheme 2. Reagents and conditions: (a) $LiBH_4$, THF, rt, 72%; (b) DMTrCl, DMAP, pyridine, rt, 90%; (c) chloro(2-cyanoethoxy)(*N*,*N*-diisopropylamino)phosphine, *i*-Pr_2NEt, THF, rt, 98%; (d) (1) succinic anhydride, DMAP, pyridine, rt; (2) CPG, WSCl, DMF, rt, 86 μmol/g.

at room temperature for 12 h and then with 1.0 M tetra-*n*-butylammonium fluoride (TBAF)/THF at room temperature for 12 h.

Please cite this article in press as: Ueno, Y. et al., *Bioorg. Med. Chem.* (2009), doi:10.1016/j.bmc.2009.01.033

The ONs that were released from the support after the treatment were purified using denaturing 20% polyacrylamide gel electrophoresis (PAGE) to afford deprotected ONs **36–77**. These ONs were analyzed by matrix-assisted laser desorption/ionization time-of-flight mass spectrometry (MALDI-TOF MS), and the observed molecular weights were in agreement with their structures.

2.3. Thermal stabilities of siRNAs

The thermal stability of siRNAs was studied by thermal denaturation in 0.01 M sodium phosphate buffer (pH 7.0) containing 0.1 M NaCl (Table 2). The melting temperatures (T_ms) of siRNAs **18**, **21**, and **24** were 79.0, 77.1, and 78.2 °C, respectively. These results showed that the thermal stabilities of siRNA **21** which contained **1** and siRNA **24** which contained **2** were lower than that of siRNA **18** with a natural dinucleotide at its overhang portion. However, the T_m values of siRNAs **18**, **21**, and **24** were not considerably different from each other.

2.4. Dual-luciferase assay

The ability of modified siRNAs to suppress gene expression was determined by a dual-luciferase assay using a psiCHECK-2 vector,

Table 1
Sequences of oligonucleotides (ONs) used in this study

Number of siRNA	No. of ON	Sequence
siRNA**16**	ON**36**	5′-GGCCUUUCACUACUCCUAC-3′
	ON**37**	3′-CCGGAAAGUGAUGAGGAUG-5′
siRNA**17**	ON**38**	5′-GGCCUUUCACUACUCCUACt-3′
	ON**39**	3′-tCCGGAAAGUGAUGAGGAUG-5′
siRNA**18**	ON**40**	5′-GGCCUUUCACUACUCCUACtt-3′
	ON**41**	3′-ttCCGGAAAGUGAUGAGGAUG-5′
siRNA**19**	ON**42**	5′-GGCCUUUCACUACUCCUACttt-3′
	ON**43**	3′-tttCCGGAAAGUGAUGAGGAUG-5′
siRNA**20**	ON**44**	5′-GGCCUUUCACUACUCCUAC**1**-3′
	ON**45**	3′-**1**CCGGAAAGUGAUGAGGAUG-5′
siRNA**21**	ON**46**	5′-GGCCUUUCACUACUCCUAC**11**-3′
	ON**47**	3′-**11**CCGGAAAGUGAUGAGGAUG-5′
siRNA**22**	ON**48**	5′-GGCCUUUCACUACUCCUAC**111**-3′
	ON**49**	3′-**111**CCGGAAAGUGAUGAGGAUG-5′
siRNA**23**	ON**50**	5′-GGCCUUUCACUACUCCUAC**2**-3′
	ON**51**	3′-**2**CCGGAAAGUGAUGAGGAUG-5′
siRNA**24**	ON**52**	5′-GGCCUUUCACUACUCCUAC**22**-3′
	ON**53**	3′-**22**CCGGAAAGUGAUGAGGAUG-5′
siRNA**25**	ON**54**	5′-GGCCUUUCACUACUCCUAC**222**-3′
	ON**55**	3′-**222**CCGGAAAGUGAUGAGGAUG-5′
siRNA**26**	ON**56**	5′-GGCCUUUCACUACUCCUAC**3**-3′
	ON**57**	3′-**3**CCGGAAAGUGAUGAGGAUG-5′
siRNA**27**	ON**58**	5′-GGCCUUUCACUACUCCUAC**33**-3′
	ON**59**	3′-**33**CCGGAAAGUGAUGAGGAUG-5′
siRNA**28**	ON**60**	5′-GGCCUUUCACUACUCCUAC**333**-3′
	ON**61**	3′-**333**CCGGAAAGUGAUGAGGAUG-5′
siRNA**29**	ON**62**	5′-AGAUCCAUACGUCCGUGAAtt-3′
	ON**63**	3′-tgUCUAGGUAUGCAGGCACUU-5′
siRNA**30**	ON**64**	5′-GCACCGGCAGGAGAUCAUAtt-3′
	ON**65**	3′-gtCGUGGCCGUCCUCUAGUAU-5′
–	ON**66**	**F**-5′-GGCCUUUCACUACUCCUACtt-3′
–	ON**67**	**F**-5′-GGCCUUUCACUACUCCUAC**11**-3′
siRNA**31**	ON**68**	5′-GUCUCGUAGACCGUGCAUCAUU-3′
	ON**69**	3′-UUCAGAGCAUCUGGCACGUAGU-5′
siRNA**32**	ON**70**	5′-GUCUCGUAGACCGUGCAUCAtt-3′
	ON**71**	3′-ttCAGAGCAUCUGGCACGUAGU-5′
siRNA**33**	ON**72**	5′-GUCUCGUAGACCGUGCAUCA**11**-3′
	ON**73**	3′-**11**CAGAGCAUCUGGCACGUAGU-5′
siRNA**34**	ON**74**	5′-GUCUCGUAGACCGUGCAUCA**12**-3′
	ON**75**	3′-**21**CAGAGCAUCUGGCACGUAGU-5′
siRNA**35**	ON**76**	5′-GUCUCAUAGGCCAUGCGUCA**11**-3′
	ON**77**	3′-**11**CAGAGUAUCCGGGACGCAGU-5′

The capital letters indicate ribonucleosides. The small italic letters represent 2′-deoxyribonucleosides. The underlined letters indicate the mismatch bases. **F** shows fluorescein.

Table 2
T_m values

siRNA	T_m (°C)
siRNA**18**	79.0
siRNA**21**	77.1
siRNA**24**	78.2

which contained *Renilla* and firefly luciferase genes. The sequences of the siRNAs were designed to target the *Renilla* luciferase gene. HeLa cells were co-transfected with the vector and indicated the amount of siRNAs. The signals of *Renilla* luciferase were normalized to those of firefly luciferase.

The results are shown in Figure 2. The silencing activities of the siRNAs possessing overhang moieties were markedly greater than those of siRNA **16**, which lacked an overhang portion. Surprisingly, the silencing activities of the siRNAs carrying aromatic compounds **1**, **2**, and **3** at their 3′-overhang regions were almost equal to those of siRNAs **17**, **18**, and **19**, which had natural thymidines at their 3′-overhang portions, at all concentrations. The number of aromatic derivatives at the overhang moieties seemed to influence the activities of the siRNAs. At all concentrations, the silencing activities of siRNAs with two aromatic compounds at their 3′-overhang regions tended to be greater than that of those carrying one or three aromatic compounds at their 3′-overhang portions. The silencing activities of the siRNAs carrying the 1,3-substituted compound **1**, the 1,2-substituted compound **2**, and the pyridine derivative **3** were not considerably different at each concentration.

Argonaute2/eIF2C2 (hAgo2) has been identified as a key protein with endonuclease activity associated with RISC in the RNAi pathway.[27,28] In order to examine whether the observed silencing activities could be attributed to RNAi, the activities of the modified siRNAs were studied after treating HeLa cells with eIF2C2-targeting siRNAs. We hypothesized that if the silencing activities of the modified siRNAs resulted from RNAi, the expression levels of luciferase proteins would recover if HeLa cells were treated with siRNAs that targeted eIF2C2. Two kinds of siRNAs targeting eIF2C2 were used in this study: one (siRNA **29**) that targeted open reading frame (ORF) positions 1168–1188 and another (siRNA **30**) that targeted ORF positions 1897–1917. HeLa cells were transfected with siRNA **29** or siRNA **30**. After incubation for 1 h, the cells were co-transfected with psiCHECK-2 vector and siRNAs modified with aromatic compounds. After incubation for 24 h, the activity of *Renilla* luciferase was measured. As shown in Figure 3, the signals of *Renilla* luciferase were recovered on treatment with siRNAs targeting eIF2C2. These results indicated that the silencing activities of modified siRNAs could be attributed to RNAi.

2.5. Nuclease-resistance

Improving the nuclease resistance of siRNA is important for the therapeutic application of synthetic siRNAs. It was expected that RNAs carrying the aromatic compounds would be more nuclease resistant than unmodified RNAs. First, the stability of the RNAs in PBS containing bovine serum was investigated. ONs **66** and **67** labeled at the 5′-ends with fluorescein were incubated in PBS containing 5% bovine serum. ON **67** contained the aromatic compound **1** at the 3′-overhang region. The reactions were analyzed with PAGE under denaturing conditions. Figure 4 shows the results. After 1 min of incubation, both the ONs were hydrolyzed completely. The results implied that ON **67**, which carried **1**, was hydrolyzed mainly by the endonuclease activity in the bovine serum.

Next, the susceptibility of the ONs to snake venom phosphodiesterase (SVPD), a 3′-exonuclease, was examined. Unmodified ON

Please cite this article in press as: Ueno, Y. et al., *Bioorg. Med. Chem.* (2009), doi:10.1016/j.bmc.2009.01.033

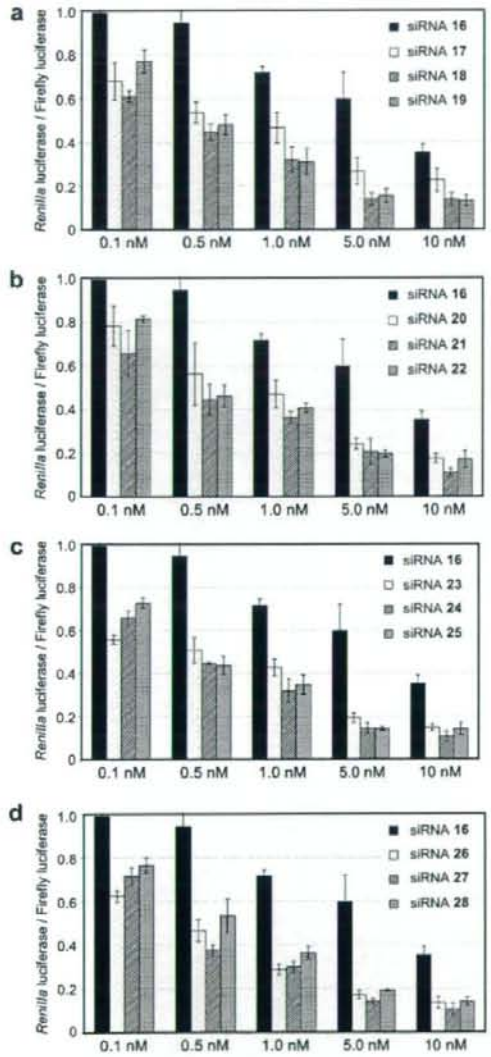

Figure 2. Dual-luciferase assay (1). The experimental conditions are as given under Section 4.

40, modified ON **46** carrying benzene derivative **1**, and modified ON **52** that contained pyridine derivative **2** were labeled with [γ-^{32}P]ATP and incubated with SVPD. The reactions were analyzed using PAGE under denaturing conditions. As shown in Figure 5, unmodified ON **40** was hydrolyzed randomly after 30 min of incubation, while modified ONs **46** and **52** were resistant to the enzyme. The half-lives ($t_{1/2}$s) of ONs **40**, **46**, and **52** were 7, 64, and 72 min, respectively. Therefore, it was apparent that ON **46** carrying benzene derivative **1** and ON **52** carrying pyridine derivative **2** were 9 and 10 times more resistant to SVPD than unmodified ON **40**.

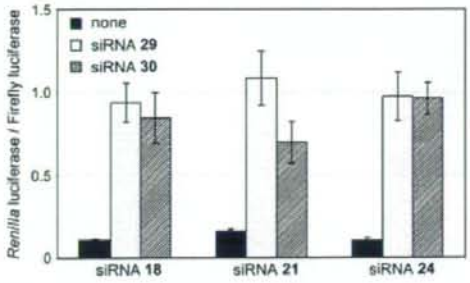

Figure 3. Dual-luciferase assay (2). HeLa cells were transfected with siRNA **29** (50 nM) or siRNA **30** (50 nM). After incubating for 1 h, the cells were co-transfected with a psiCHECK-2 vector and the modified siRNAs (10 nM). After incubating for 24 h, the activity of *Renilla* luciferase was measured. The experimental conditions are as given under Section 4.

Figure 4. 20% PAGE of ONs incubated in PBS containing 5% bovine serum: (a) ON**66**; (b) ON**67**. ONs were incubated for 0 min (lane 1), 1 min (lane 2), 3 min (lane 3), 15 min (lane 4), 1 h (lane 5), 3 h (lane 6), 6 h (lane 7), and 12 h (lane 8). The experimental conditions are as given under Section 4.

2.6. Inhibition of HCV replication

It has been reported that hepatitis C virus (HCV) replication is efficiently suppressed by siRNA **31** that targets an internal ribosome entry site (IRES) region of HCV.[35] Accordingly, in order to examine the efficacy of the modified siRNAs, we compared the abilities of the modified siRNAs to suppress HCV replication with those of normal siRNAs. The sequences of the siRNAs used in this study are listed in Table 1. The siRNAs **32**, **33**, and **34** contained thymidines, benzene derivatives, and benzene and pyridine derivatives at their 3′-overhang regions, respectively. siRNA **35** contained 4 mismatched bases in its sequence.

Figure 6 shows the results. siRNAs **32**, **33**, and **34** dose-dependently inhibited HCV replication. They almost completely suppressed HCV replication at a concentration of 100 pM, while the replication ratio of the siRNA**35**, which contained the mismatched bases, was 75% at the same concentration. The siRNAs exerted no cytotoxic effect at 100 pM concentrations (Fig. 6c and d). Thus, it was found that modified siRNAs **33** and **34** suppress HCV replication in a sequence-specific manner. At each concentration, the replication ratios of HCV in cells treated with siRNAs **33** and **34**, which carried aromatic compounds at their 3′-overhang regions, were almost equal to the ratio in the cells treated with siRNAs **31** and **32** with natural uridines and thymidines at their 3′-overhang portions. These results indicated that the silencing abilities of the modified siRNAs are almost equal to those of the normal siRNA, which had natural nucleosides at their 3′-overhang regions.

Please cite this article in press as: Ueno, Y. et al., *Bioorg. Med. Chem.* (2009), doi:10.1016/j.bmc.2009.01.033

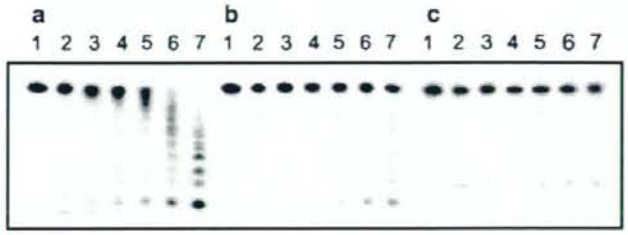

Figure 5. 20% PAGE of 5′-^{32}P-labeled ONs hydrolyzed by SVPD: (a) ON**40**, (b) ON**46**, (c) ON**52**. ONs were incubated with SVPD for 0 min (lane 1), 1 min (lane 2), 3 min (lane 3), 5 min (lane 4), 10 min (lane 5), 30 min (lane 6), and 60 min (lane 7). The experimental conditions are as described in Section 4.

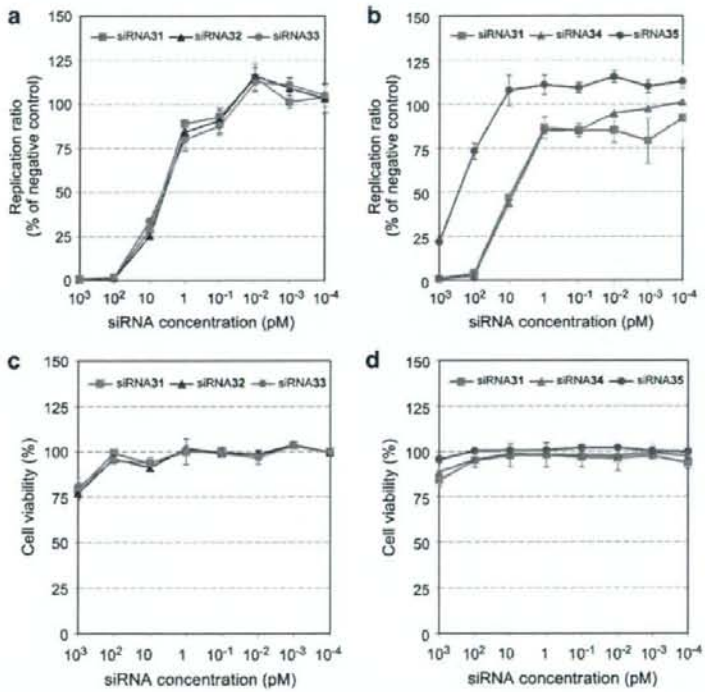

Figure 6. Effect of siRNAs on HCV replication. (a) and (b): Inhibition of HCV replication by siRNAs in R6FLR-N replicon cells. HCV replication was calculated by measuring the luminescence ratio with a Bright-Glo luciferase assay system. (c) and (d): Cell viability was determined by a WST-8 assay. Data are represented as mean ± SD ($n = 3$). The experimental conditions are as described in Section 4.

3. Discussion and conclusions

We designed and synthesized siRNAs possessing the aromatic compounds, 1,3-bis(hydroxymethyl)benzene, 1,3-bis(hydroxymethyl)pyridine, and 1,2-bis(hydroxymethyl)benzene at their 3′-overhang regions. RNAs containing these aromatic compounds at their 3′-ends were successfully synthesized by the phosphoramidite method by using a DNA/RNA synthesizer. It has been reported that the overhang nucleosides of RNA/RNA duplexes influence the thermal stabilities of the RNA/RNA duplexes.[36] Therefore, the thermal stability of the siRNAs was studied using thermal denaturation analysis. It was found that although the thermal stability of siRNA **21**, which contained 1,3-bis(hydroxymethyl)benzene, and siRNA **24**, which contained 1,3-bis(hydroxymethyl)pyridine, is slightly lower than that of siRNA **18**, which had a natural dinucleotide at the overhang portion, the T_m values of these three siRNA were not considerably different. Therefore, it was considered that the change in the thermal stability of the siRNAs, caused by the introduction of aromatic residues, influenced the silencing activities of the siRNAs to a very small extent.

The silencing activities of the siRNAs were examined by dual-luciferase assay using the psiCHECK-2 vector. It was revealed that the modified siRNAs were more potent than the siRNAs without the 3′-overhang regions. Moreover, the silencing activities of the

Please cite this article in press as: Ueno, Y. et al., *Bioorg. Med. Chem.* (2009), doi:10.1016/j.bmc.2009.01.033

modified siRNAs were almost equal to those of the normal siRNAs. It has been reported that in the RNAi machinery, the 3′-overhang region of the guide strand (the antisense strand) of siRNA is recognized by a PAZ domain, and the 2-nt 3′-overhang is accommodated into a binding pocket composed of hydrophobic amino acids; this pocket is located in the domain.[29–32] In this report, we tested the siRNAs with the monocyclic compounds at their 3′-overhang regions. They showed silencing activities similar to those of unmodified siRNAs. Therefore, it is considered that recognition of the 3′-overhang portions of the siRNAs by the PAZ domain of human Argonaute is not so stringent. It has been reported that the 2-nt 3′-overhang was the most efficient in an experiment using 21-nt siRNA in *Drosophila* embryo lysate.[33] The silencing activity of the siRNAs with two aromatic compounds at their 3′-overhang regions also tended to be greater than that of carrying one or three aromatic compounds in this experiment.

It has been reported that pre-treatment of tissue culture cells with siRNAs can inhibit the replication of a large number of viruses.[37] Therefore, we examined the inhibition activity of the modified siRNAs using the cells harboring HCV replicons. It was found that the modified siRNAs suppressed HCV replication in a sequence-specific manner. The replication ratios of HCV in cells treated with siRNAs carrying aromatic compounds at their 3′-overhang regions were almost equal to those treated with siRNAs with natural nucleosides at their 3′-overhang portions. Therefore, siRNAs possessing aromatic compounds at their 3′-overhang region can be used to inhibit HCV replication.

An improvement in nuclease resistance of siRNA is important for the therapeutic application of synthetic siRNA.[4–6] We examined the susceptibility of the RNAs possessing aromatic compounds at their 3′-ends. SVPD was used as the model 3′-exonuclease, and the stability of the RNAs in bovine serum was also studied. The 3′-modified RNAs were hydrolyzed completely by the endonuclease activity in the bovine serum after 1 min of incubation. In contrast, the 3′-modification was effective for improving resistance to SVPD, a 3′-exonuclease.

In summary, we synthesized the siRNAs possessing the aromatic compounds at their 3′-overhang regions. It was revealed that the modified siRNAs were more potent than the siRNAs without 3′-overhang regions and that the modified siRNAs had silencing activity similar to those of the siRNAs possessing the natural nucleosides at their 3′-overhang portions. Moreover, the modified RNAs were more resistant to 3′-exonuclease than the natural RNAs. The aromatic compounds described in this report do not have functional groups capable of forming hydrogen bonds with nucleobases. Therefore, they can be used as universal overhang units in order to improve the nuclease resistance of siRNAs.

4. Experimental

4.1. General remarks

NMR spectra were recorded at 400 MHz (^{1}H) and at 100 MHz (^{13}C), and are reported in ppm downfield from tetramethylsilane. Coupling constants (J) are expressed in Hertz. Mass spectra were obtained by electron impact (EI) or fast atom bombardment (FAB). Thin-layer chromatography was performed using Merck coated plates $60F_{254}$. Silica gel column chromatography was carried out on Wako gel C-300. siRNAs directed against eIF2C2 (hAgo2) were purchased from QIAGEN Inc.

4.1.1. 1,3-Bis(hydroxymethyl)benzene (1)

A mixture of dimethyl isophtalate (2.00 g, 10.3 mmol) and $LiBH_4$ (1.12 g, 51.5 mmol) in THF (52 mL) was stirred at room temperature for 23 h. Aqueous $NaHCO_3$ (10 mL) was added to the mixture at 0 °C, and the whole was stirred at room temperature for 1 h. The solvent was evaporated in vacuo, and the resulting residue was purified by column chromatography (SiO_2, EtOAc) to give **1** (1.36 g, 9.84 mmol) in 95% yield: ^{1}H NMR ($CDCl_3$) δ 7.39–7.26 (m, 4H), 4.71 (s, 4H); ^{13}C NMR ($CDCl_3$) δ 141.2, 128.7, 126.2, 125.5, 65.1; LRMS (EI) m/z 138 (M^+); HRMS (EI) calcd for $C_8H_{10}O_2$ 138.0681, found 138.0677. Anal. Calcd for $C_8H_{10}O_2$: C, 69.54; H, 7.30. Found: C, 69.45; H, 7.23.

4.1.2. 1-(4,4′-Dimethoxytrityloxymethyl)-3-(hydroxymethyl) benzene (6)

A mixture of **1** (0.50 g, 3.62 mmol), DMTrCl (1.23 g, 3.62 mmol), and DMAP (22 mg, 0.18 mmol) in pyridine (18 mL) was stirred at room temperature for 17 h. The mixture was partitioned between EtOAc and aqueous $NaHCO_3$ (saturated). The organic layer was washed with brine, dried (Na_2SO_4), and concentrated. The residue was purified by column chromatography (SiO_2, 20% EtOAc in hexane) to give **6** (0.82 g, 1.86 mmol) in 51% yield: ^{1}H NMR ($CDCl_3$) δ 7.52–6.82 (m, 17H), 4.70 (s, 2H), 4.18 (s, 2H), 3.80 (s, 6H); ^{13}C NMR ($CDCl_3$) δ 158.4, 145.0, 140.8, 139.7, 136.2, 130.1, 128.5, 128.2, 127.8, 126.7, 126.3, 125.7, 125.6, 113.1, 86.4, 65.4, 55.2; LRMS (EI) m/z 440 (M^+); HRMS (EI) calcd for $C_{29}H_{28}O_4$ 440.1988, found 440.1981. Anal. Calcd for $C_{29}H_{28}O_4 \cdot 1/5H_2O$: C, 78.27; H, 6.45. Found: C, 78.33; H, 6.59.

4.1.3. 1-[(2-Cyanoethyloxy)(*N*,*N*-diisopropylamino)phosphinyloxymethyl]-3-(4,4′-dimethoxytrityloxymethyl)benzene (8)

A mixture of **6** (0.35 g, 0.80 mmol), *N*,*N*-diisopropylethylamine (0.40 mL, 4.00 mmol), and chloro(2-cyanoethoxy)(*N*,*N*-diisopropylamino)phosphine (0.29 mL, 1.60 mmol) in THF (8 mL) was stirred at room temperature for 1 h. The mixture was partitioned between EtOAc and aqueous $NaHCO_3$ (saturated). The organic layer was washed with brine, dried (Na_2SO_4), and concentrated. The residue was purified by column chromatography (a neutralized SiO_2, 50% EtOAc in hexane) to give **8** (0.48 g, 0.75 mmol) in 94% yield: ^{31}P NMR ($CDCl_3$) δ 148.8; LRMS (FAB) m/z 641 (MH^+); HRMS (FAB) calcd for $C_{38}H_{46}N_2O_5P$: 641.3144, found: 6410.3129.

4.1.4. 2,6-Bis(hydroxymethyl)pyridine (2)

Dimethyl 2,6-pyridinedicarboxylate (2.00 g, 10.3 mmol) was treated as described in the preparation of **1** to give **2** (0.40 g, 2.88 mmol) in 28%: ^{1}H NMR ($CDCl_3$) δ 7.70 (t, 1H, J = 8.0), 7.19 (d, 2H, J = 8.0), 4.79 (s, 4H); ^{13}C NMR ($CDCl_3$) δ 158.4, 137.4, 119.1, 64.3; LRMS (FAB) m/z 140 (MH^+); HRMS (FAB) calcd for $C_7H_{10}NO_2$ 140.0712, found 140.0705. Anal. Calcd for $C_7H_9NO_2$: C, 60.42; H, 6.52; N, 10.07. Found: C, 60.28; H, 6.50; N, 9.95.

4.1.5. 2-(4,4′-Dimethoxytrityloxymethyl)-6-(hydroxymethyl) pyridine (7)

Compound **2** (0.50 g, 3.59 mmol) was treated as described in the preparation of **6** to give **7** (0.81 g, 1.83 mmol) in 51%: ^{1}H NMR ($CDCl_3$) δ 7.76–6.82 (m, 16H), 4.69 (s, 2H), 4.34 (s, 2H), 3.79 (s, 6H); ^{13}C NMR ($CDCl_3$) δ 158.5, 158.4, 157.6, 144.8, 137.3, 135.9, 130.0, 128.1, 127.9, 126.9, 119.4, 118.6, 113.2, 86.7, 66.6, 63.6, 55.20; LRMS (FAB) m/z 442 (MH^+); HRMS (FAB) calcd for $C_{28}H_{28}NO_4$: 442.2018, found: 442.2033.

4.1.6. 1-[(2-Cyanoethyloxy)(*N*,*N*-diisopropylamino)phosphinyloxymethyl]-3-(4,4′-dimethoxytrityloxymethyl)pyridine (9)

Compound **7** (0.20 g, 0.45 mmol) was phosphitylated as described in the preparation of **8** to give **9** (0.27 g, 0.42 mmol) in 93%: ^{31}P NMR ($CDCl_3$) δ 149.1; LRMS (FAB) m/z 642 (MH^+); HRMS (FAB) calcd for $C_{37}H_{45}N_3O_5P$: 642.3097, found: 642.3116.

Please cite this article in press as: Ueno, Y. et al., *Bioorg. Med. Chem.* (2009), doi:10.1016/j.bmc.2009.01.033

4.1.7. 1,2-Bis(hydroxymethyl)benzene (3)

Dimethyl phthalate (2.00 g, 10.3 mmol) was treated as described in the preparation of **1** to give **3** (1.02 g, 7.38 mmol) in 72%: ^{1}H NMR ($CDCl_3$) δ 7.30 (s, 4H), 4.65 (s, 4H); ^{13}C NMR ($CDCl_3$) δ 139.3, 129.6, 128.5, 63.9; LRMS (FAB) *m/z* 139 (MH^+); HRMS (FAB) calcd for $C_8H_{11}O_2$ 139.0765, found 139.0759. Anal. Calcd for $C_8H_{10}O_2$: C, 69.54; H, 7.30. Found: C, 69.75; H, 7.32.

4.1.8. 1-(4,4′-Dimethoxytrityloxymethyl)-2-(hydroxymethyl) benzene (13)

Compound **3** (0.50 g, 3.62 mmol) was treated as described in the preparation of **6** to give **13** (1.44 g, 3.27 mmol) in 90%: ^{1}H NMR ($CDCl_3$) δ 7.50–6.85 (m, 17H), 4.43 (d, 2H, J = 6.0), 4.18 (s, 2H), 3.79 (s, 6H); ^{13}C NMR ($CDCl_3$) δ 158.6, 144.5, 140.5, 136.4, 135.7, 129.9, 129.8, 129.5, 128.6, 128.1, 127.9, 126.9, 113.4, 87.6, 65.2, 63.6, 55.2; LRMS (EI) *m/z* 440 (M^+); HRMS (EI) calcd for $C_{29}H_{28}O_4$ 440.1988, found 440.1991. Anal. Calcd for $C_{29}H_{28}O_4 \cdot 1/5H_2O$: C, 78.27; H, 6.45. Found: C, 78.24; H, 6.61.

4.1.9. 1-[(2-Cyanoethyloxy)(*N*,*N*-diisopropylamino)phosphinyloxymethyl]-2-(4,4′-dimethoxytrityloxymethyl)benzene (14)

Compound **13** (0.35 g, 0.80 mmol) was phosphitylated as described in the preparation of **8** to give **14** (0.50 g, 0.78 mmol) in 98%: ^{31}P NMR ($CDCl_3$) δ 148.4; LRMS (FAB) *m/z* 641 (MH^+); HRMS (FAB) calcd for $C_{38}H_{46}N_2O_5P$: 641.3144, found: 641.3127.

4.2. Solid support synthesis

A mixture of **1** (0.30 g, 0.68 mmol), succinic anhydride (0.20 g, 2.04 mmol), and DMAP (4 mg, 0.03 mmol) in pyridine (6.8 mL) was stirred at room temperature. After 24 h, the solution was partitioned between $CHCl_3$ and H_2O, and the organic layer was washed with H_2O and brine. The separated organic phase was dried (Na_2SO_4) and concentrated to give a succinate. Aminopropyl controlled pore glass (0.50 g, 0.11 mmol) was added to a solution of the succinate and WSCI (0.11 g, 0.57 mmol) in DMF (10 mL), and the mixture was kept for 72 h at room temperature. After the resin was washed with pyridine, a capping solution (6 mL, 0.1 M DMAP in pyridine:Ac_2O = 9:1, v/v) was added and the whole mixture was kept for 24 h at room temperature. The resin was washed with MeOH and acetone, and dried in vacuo. Amount of loaded compound **1** to solid support was 108 μmol/g from calculation of released dimethoxytrityl cation by a solution of 70% $HClO_4$:EtOH (3:2, v/v). In a similar manner, solid supports with **2** and **3** were obtained in 74 and 86 μmol/g loading amounts, respectively.

4.3. RNA synthesis

Synthesis was carried out with a DNA/RNA synthesizer by phosphoramidite method. Deprotection of bases and phosphates was performed in concentrated NH_4OH:EtOH (3:1, v/v) at room temperature for 12 h. 2′-TBDMS groups were removed by 1.0 M tetrabutylammonium fluoride (TBAF, Aldrich) in THF at room temperature for 12 h. The reaction was quenched with 0.1 M TEAA buffer (pH 7.0) and desalted on a Sep-Pak C18 cartridge. Deprotected ONs were purified by 20% PAGE containing 7 M urea to give the highly purified ON**44** (8), ON**45** (8), ON**46** (8), ON**47** (12), ON**48** (5), ON**49** (6), ON**50** (28), ON**51** (28), ON**52** (29), ON**53** (14), ON**54** (35), ON**55** (20), ON**56** (11), ON**57** (4), ON**58** (5), ON**59** (7), ON**60** (3), ON**61** (2), ON**66** (20), ON**67** (11), ON**72** (14), ON**73** (14), ON**74** (33), ON**75** (37), ON**76** (21), ON**77** (19). The yields are indicated in parentheses as OD units at 260 nm starting from 1.0 μmol scale. Extinction coefficients of the ONs were calculated from those of mononucleotides and dinucleotides according to the nearest-neighbor approximation method.[38]

4.4. MALDI-TOF/MS analysis of RNAs

Spectra were obtained with a time-of-flight mass spectrometer. ON**44**: calculated mass, 6094.6; observed mass, 6086.2. ON**45**: calculated mass, 6403.9; observed mass, 6397.7. ON**46**: calculated mass, 6294.8; observed mass, 6294.4. ON**47**: calculated mass, 6604.0; observed mass, 6605.6. ON**48**: calculated mass, 6494.9; observed mass, 6489.2. ON**49**: calculated mass, 6804.1; observed mass, 6797.1. ON**50**: calculated mass, 6095.6; observed mass, 6096.8. ON**51**: calculated mass, 6404.9; observed mass, 6405.0. ON**52**: calculated mass, 6296.6; observed mass, 6296.1. ON**53**: calculated mass, 6605.8; observed mass, 6603.5. ON**54**: calculated mass, 6497.9; observed mass, 6503.5. ON**55**: calculated mass, 6807.1; observed mass, 6807.2. ON**56**: calculated mass, 6094.6; observed mass, 6092.2. ON**57**: calculated mass, 6403.9; observed mass, 6399.1. ON**58**: calculated mass, 6294.8; observed mass, 6290.4. ON**59**: calculated mass, 6604.0; observed mass, 6603.7. ON**60**: calculated mass, 6494.9; observed mass, 6492.7. ON**61**: calculated mass, 6804.2; observed mass, 6806.8. ON**66**: calculated mass, 7070.4; observed mass, 7067.5. ON**67**: calculated mass, 6862.3; observed mass, 6856.9. ON**72**: calculated mass, 6739.9; observed mass, 6731.8. ON**73**: calculated mass, 6802.9; observed mass, 6794.6. ON**74**: calculated mass, 6740.9; observed mass, 6734.9. ON**75**: calculated mass, 6803.9; observed mass, 6797.9. ON**76**: calculated mass, 6739.9; observed mass, 6734.2. ON**77**: calculated mass, 6802.9; observed mass, 6794.7.

4.5. Thermal denaturation study

Each solution containing each siRNA (3 μM) in a buffer composed of 10 mM Na_2HPO_4/NaH_2PO_4 (pH 7.0) and 100 mM NaCl was heated at 95 °C for 3 min, then cooled gradually to an appropriate temperature, and used for the thermal denaturation studies. Thermal-induced transitions of each mixture were monitored at 260 nm with a spectrophotometer.

4.6. Dual-luciferase assay

HeLa cells were grown at 37 °C in a humidified atmosphere of 5% CO_2 in air in Minimum Essential Medium (MEM) (Invitrogen) supplemented with 10% fetal bovine serum (FBS). Twenty-four hours before transfection, HeLa cells (4×10^4/mL) were transferred to 96-well plates (100 μL per well). They were transfected, using TransFast (Promega), according to instructions for transfection of adherent cell lines. Cells in each well were transfected with a solution (35 μL) of 20 ng of psiCHECK-2 vector (Promega), the indicated amounts of siRNAs, and 0.3 μg of TransFast in Opti-MEM I Reduced-Serum Medium (Invitrogen), and incubated at 37 °C. Transfection without siRNA was used as a control. After 1 h, MEM (100 μL) containing 10% FBS and antibiotics was added to each well, and the whole was further incubated at 37 °C. After 24 h, cell extracts were prepared in Passive Lysis Buffer (Promega). Activities of firefly and *Renilla* luciferases in cell lysates were determined with a dual-luciferase assay system (Promega) according to a manufacturer's protocol. The results were confirmed by at least three independent transfection experiments with two cultures each and are expressed as the average from four experiments as mean ± SD.

4.7. Stability of ON in the PBS containing bovine serum

Each ON (600 pmol) labeled with fluorescein at 5′-end was incubated in PBS (300 μL) containing 5% bovine serum at 37 °C. At appropriate periods, aliquots (5 μL) of the reaction mixture were separated and added to a solution of 9 M urea (15 μL). The mixtures were analyzed by electrophoresis on 20% polyacrylamide

Please cite this article in press as: Ueno, Y. et al., *Bioorg. Med. Chem.* (2009), doi:10.1016/j.bmc.2009.01.033

gel containing 7 M urea. The labeled ON in the gel was visualized by a Typhoon system (Amersham Biosciences).

4.8. Partial hydrolysis of ONs with snake venom phosphodiesterase

Each ON (100 pmol) labeled with ^{32}P at the 5′-end was incubated with snake venom phosphodiesterase (3 ng) in a buffer containing 37.5 mM Tris-HCl (pH 7.0) and 7.5 mM $MgCl_2$ (total 40 μL) at 37 °C. At appropriate periods, aliquots (5 μL) of the reaction mixture were separated and added to a solution of 9 M urea (10 μL). The mixtures were analyzed by electrophoresis on 20% polyacrylamide gel containing 7 M urea. Densities of radioactivity of the gel were visualized by a Bio-imaging analyzer (Bas 2000, Fuji Co., Ltd).

4.9. Subgenomic HCV replicon cells

Subgenomic HCV replicon cells (R6FLR-N) were conditional expression system of the HCV-non-structure region and luciferase gene. These cells were cultured in DMEM-GlutaMAX High glucose (GIBCO) supplemented with 10% FBS, 1 unit penicillin (GIBCO), 100 μg/ml streptomycin (GIBCO), and 500 μg/ml G418 (GIBCO).

4.10. Transfection and evaluation of virus replication

Six kinds of siRNAs were used in this investigation. The siControl Non-Targeting siRNA (product No. D-001210-03-05; Dharmacon Inc.) was used as a negative control. The siRNA**31** was used as a positive control.[35] The subgenomic HCV replicon cells (R6FLR-N) were transfected with the siRNAs by reverse transfection. The cells were plated in 96-well plate (Falcon) at a density of 4×10^3 cells/well. Each siRNA (100 aM ~ 1 nM) was transfected to the cells using Lipofectamine RNAiMAX (Invitrogen) and Opti-MEM (GIBCO-BRL). The cells were incubated for 72 h after being transfected with siRNAs. HCV replication was evaluated by luminescence in a Mithras LB940 (Berthold Technologies, Wildbad, Germany) using Bright-Glo Luciferase Assay System (Promega) according to the manufacturer's protocol.

4.11. Cell viability

In order to evaluate cytotoxic effects of the siRNAs, cell viabilities were measured by metabolic conversion of 2-(2-methoxy-4-nitrophenyl)-3-(4-nitrophenyl)-5-(2,4-disulfophenyl)-2H-tetrazolium, monosodium salt (WST-8) using a Cell Counting Kit-8 (Dojindo, Kumamoto, Japan) according to the manufactuer's protocol.

Acknowledgments

This work was supported by a Grant from Precursory Research for Embryonic Science and Technology (PRESTO) of the Japan Science and Technology Agency (JST) and a Grant-in-Aid for Scientific Research from the Japan Society for the Promotion of Science (JSPS). We are grateful to Professor Y. Tomari (the University of Tokyo) for his helpful advice. We are also grateful to Professor Y. Hirata (Gifu University) and Professor K. Kiuchi (Gifu University) for providing technical assistance in the dual-luciferase assay.

References and notes

1. Fire, A.; Xu, S.; Montgomery, M. K.; Kostas, S. A.; Driver, S. E.; Mello, C. C. *Nature* **1998**, *391*, 806.
2. Elbashir, S. M.; Harborth, J.; Lendeckel, W.; Yalcin, A.; Weber, K.; Tuschl, T. *Nature* **2001**, *411*, 494.
3. Elbashir, S. M.; Lendeckel, W.; Tuschl, T. *Genes Dev.* **2001**, *15*, 188.
4. Bumcrot, D.; Manoharan, M.; Koteliansky, V.; Sah, D. W. Y. *Nat. Chem. Biol.* **2006**, *2*, 711.
5. Behlke, M. A. *Mol. Ther.* **2006**, *13*, 644.
6. Kim, D. A.; Rossi, J. J. *Nat. Rev. Genet.* **2007**, *8*, 173.
7. Hamada, M.; Ohtsuka, T.; Kawaida, R.; Koizumi, M.; Morita, K.; Furukawa, H.; Imanishi, T.; Miyagishi, M.; Taira, K. *Antisense Nucleic Acid Drug Dev.* **2002**, *12*, 301.
8. Harborth, J.; Elbashir, S. M.; Vandenburgh, K.; Manninga, H.; Scaringe, S. A.; Weber, K.; Tuschl, T. *Antisense Nucleic Acid Drug Dev.* **2003**, *13*, 83.
9. Chiu, Y.-L.; Rana, T. M. *Mol. Cell* **2002**, *10*, 549.
10. Chiu, Y.-L.; Rana, T. M. *RNA* **2003**, *9*, 1034.
11. Braasch, D. A.; Jensen, S.; Liu, Y.; Kaur, K.; Arar, K.; White, M. A.; Corey, D. R. *Biochemistry* **2003**, *42*, 7967.
12. Amarzguioui, M.; Holen, T.; Babaie, E.; Prydz, H. *Nucleic Acids Res.* **2003**, *31*, 589.
13. Czauderna, F.; Fechtner, M.; Dames, S.; Aygün, H.; Klippel, A.; Pronk, G. J.; Giese, K.; Kaufmann, J. *Nucleic Acids Res.* **2003**, *31*, 2705.
14. Grünweller, A.; Wyszko, E.; Bieber, B.; Jahnel, R.; Erdmann, V. A.; Kurreck, J. *Nucleic Acids Res.* **2003**, *31*, 3185.
15. Hall, A. H. S.; Wan, J.; Shaughnessy, E. E.; Shaw, B. R.; Alexander, K. A. *Nucleic Acids Res.* **2004**, *32*, 5991.
16. Hall, A. H. S.; Wan, J.; Spesock, A.; Sergueeva, Z.; Shaw, B. R.; Alexander, K. A. *Nucleic Acids Res.* **2006**, *34*, 2773.
17. Prakash, T. P.; Allerson, C. R.; Dande, P.; Vickers, T. A.; Sioufi, N.; Jarres, R.; Baker, B. F.; Swayze, E. E.; Griffey, R. H.; Bhat, B. *J. Med. Chem.* **2005**, *48*, 4247.
18. Hoshika, S.; Minakawa, N.; Kamiya, H.; Harashima, H.; Matsuda, A. *FEBS Lett.* **2005**, *579*, 3115.
19. Elmén, J.; Thoberg, H.; Ljungberg, K.; Frieden, M.; Westergaard, M.; Xu, Y.; Wahren, B.; Liang, Z.; Ørum, H.; Koch, T.; Wahlestedt, C. *Nucleic Acids Res.* **2005**, *33*, 439.
20. Dowler, T.; Bergeron, D.; Tedeschi, A.-L.; Paquet, L.; Ferrari, N.; Damha, M. J. *Nucleic Acids Res.* **2006**, *34*, 1669.
21. Watts, J. K.; Choubdar, N.; Sadalapure, K.; Robert, F.; Wahba, A. S.; Pelletier, J.; Pinto, B. M.; Damha, M. J. *Nucleic Acids Res.* **2007**, *35*, 1441.
22. Choung, S.; Kim, Y. J.; Kim, S.; Park, H.-O.; Choi, Y.-C. *Biochem. Biophys. Res. Commun.* **2006**, *342*, 919.
23. Abe, N.; Abe, H.; Ito, Y. *J. Am. Chem. Soc.* **2007**, *129*, 15108.
24. Fisher, M.; Abramov, M.; Aerschot, A. V.; Xu, D.; Juliano, R. L.; Herdewijn, P. *Nucleic Acids Res.* **2007**, *35*, 1064.
25. Bramsen, J. B.; Laursen, M. B.; Damgaard, C. K.; Lena, S. W.; Babu, B. R.; Wengel, J.; Kjems, J. *Nucleic Acids Res.* **2007**, *35*, 5886.
26. Odadzic, D.; Bramsen, J. B.; Smicius, R.; Bus, C.; Kjems, J.; Engels, J. W. *Bioorg. Med. Chem.* **2008**, *16*, 518.
27. Hammond, S. M.; Boettcher, S.; Caudy, A. A.; Kobayashi, R.; Hannon, G. J. *Science* **2001**, *293*, 1146.
28. Martinez, J.; Patkaniowska, A.; Urlaub, H.; Lührmann, R.; Tuschl, T. *Cell* **2002**, *110*, 563.
29. Lingel, A.; Simon, B.; Izaurralde, E.; Sattler, M. *Nature* **2003**, *426*, 465.
30. Yan, K. S.; Yan, S.; Farooq, A.; Han, A.; Zeng, L.; Zhou, M.-M. *Nature* **2003**, *426*, 469.
31. Song, J.-J.; Liu, J.; Tolia, N. H.; Schneiderman, J.; Smith, S. K.; Martienssen, R. A.; Hannon, G. J.; Joshua-Tor, L. *Nat. Struct. Biol.* **2003**, *12*, 1026.
32. Ma, J. B.; Te, K.; Patel, D. J. *Nature* **2004**, *429*, 318.
33. Elbashir, S. M.; Martinez, J.; Patkaniowska, A.; Lendeckel, W.; Tuschl, T. *EMBO J.* **2001**, *20*, 6877.
34. Sinha, N. D.; Biernat, J.; Köester, H. *Tetrahedron Lett.* **1983**, *24*, 5843.
35. Watanabe, T.; Sudoh, M.; Miyagishi, M.; Akashi, H.; Arai, M.; Inoue, K.; Taira, K.; Yoshida, M.; Kohara, M. *Gene Ther.* **2006**, *13*, 883.
36. Ohmichi, T.; Nakano, S.; Miyoshi, D.; Sugimoto, N. *J. Am. Chem. Soc.* **2002**, *124*, 10367.
37. Van Rij, R. P.; Andino, R. *Trends Biotechnol.* **2006**, *24*, 186.
38. Puglisi, J. D.; Tinoco, I., Jr.. In *Methods in Enzymology*; Dahlberg, J. E., Abelson, J. N., Eds.; Academic: San Diego, 1989; Vol. 180, pp 304–325.

Please cite this article in press as: Ueno, Y. et al., *Bioorg. Med. Chem.* (2009), doi:10.1016/j.bmc.2009.01.033

JOURNAL OF VIROLOGY, Mar. 2009, p. 2338–2348 Vol. 83, No. 5
0022-538X/09/$08.00+0 doi:10.1128/JVI.01840-08

Arsenic Trioxide Inhibits Hepatitis C Virus RNA Replication through Modulation of the Glutathione Redox System and Oxidative Stress[▽]

Misao Kuroki,[1] Yasuo Ariumi,[1] Masanori Ikeda,[1] Hiromichi Dansako,[1] Takaji Wakita,[2] and Nobuyuki Kato[1]*

Department of Tumor Virology, Okayama University Graduate School of Medicine, Dentistry, and Pharmaceutical Sciences, 2-5-1, Shikata-cho, Okayama 700-8558, Japan,[1] and Department of Virology II, National Institute of Infectious Diseases, 1-23-1 Toyama, Shinjuku-ku, Tokyo 162-8640, Japan[2]

Received 2 September 2008/Accepted 13 December 2008

Arsenic trioxide (ATO), a therapeutic reagent used for the treatment of acute promyelocytic leukemia, has recently been reported to increase human immunodeficiency virus type 1 infectivity. However, in this study, we have demonstrated that replication of genome-length hepatitis C virus (HCV) RNA (O strain of genotype 1b) was notably inhibited by ATO at submicromolar concentrations without cell toxicity. RNA replication of HCV-JFH1 (genotype 2a) and the release of core protein into the culture supernatants were also inhibited by ATO after the HCV infection. To clarify the mechanism of the anti-HCV activity of ATO, we examined whether or not PML is associated with this anti-HCV activity, since PML is known to be a target of ATO. Interestingly, we observed the cytoplasmic translocation of PML after treatment with ATO. However, ATO still inhibited the HCV RNA replication even in the PML knockdown cells, suggesting that PML is dispensable for the anti-HCV activity of ATO. In contrast, we found that *N*-acetyl-cysteine, an antioxidant and glutathione precursor, completely and partially eliminated the anti-HCV activity of ATO after 24 h and 72 h of treatment, respectively. In this context, it is worth noting that we found an elevation of intracellular superoxide anion radical, but not hydrogen peroxide, and the depletion of intracellular glutathione in the ATO-treated cells. Taken together, these findings suggest that ATO inhibits the HCV RNA replication through modulation of the glutathione redox system and oxidative stress.

Hepatitis C virus (HCV) is the causative agent of chronic hepatitis, which progresses to liver cirrhosis and hepatocellular carcinoma. HCV is an enveloped virus with a positive single-stranded 9.6-kb RNA genome, which encodes a large polyprotein precursor of approximately 3,000 amino acid residues. This polyprotein is cleaved by a combination of the host and viral proteases into at least 10 proteins in the following order: core, envelope 1 (E1), E2, p7, nonstructural 2 (NS2), NS3, NS4A, NS4B, NS5A, and NS5B (30).

Alpha interferon has been used as an effective anti-HCV reagent in clinical therapy for patients with chronic hepatitis C. The current combination treatment with pegylated alpha interferon and ribavirin, a nucleoside analogue, has been shown to improve the sustained virological response rate to more than 50% (15). However, the adverse effects of the combination therapy and the limited efficacy against genotype 1b warrant the development of new anti-HCV reagents.

Arsenic trioxide (ATO) (As_2O_3, arsenite) has been used as a therapeutic reagent in acute promyelocytic leukemia, which bears an oncogenic PML-retinoic acid receptor alpha fusion protein resulting from chromosomal translocation (51, 52, 68, 70). The ATO treatment induces complete remission through degradation of the aberrant PML-retinoic acid receptor α (70). The PML tumor suppressor protein is required for formation of the PML nuclear body (PML-NB), also known as nuclear dot 10 or the PML oncogenic domain, which is often disrupted by infection with DNA viruses, such as herpes simplex virus type 1, human cytomegalovirus, and Epstein-Barr virus (17). The treatment with ATO results in degradation of the PML protein and disruption of the PML-NB (70). Therefore, ATO has been become a useful probe for investigating the functions of the PML-NB, including cell growth, apoptosis, stress response, and viral infection. Indeed, ATO has been shown to increase retroviral infectivity, such as human immunodeficiency virus type 1 (HIV-1) and murine leukemia virus infectivity, but the mechanisms of this change are not well understood (5, 6, 32, 44, 47, 50, 57). In contrast, ATO was recently reported to inhibit the replication of HCV subgenomic replicon RNA (24). However, it also remains unclear how ATO inhibits the HCV RNA replication. In this study, using genome-length HCV RNA replication systems, we investigated the molecular mechanism(s) of the anti-HCV activity of ATO, and we provide evidence that ATO inhibits HCV RNA replication through modulation of the glutathione redox system and oxidative stress.

MATERIALS AND METHODS

Reagents. ATO, *N*-acetyl-cysteine (NAC), ascorbic acid (vitamin C), and L-buthionine sulfoximine (BSO) were purchased from Sigma (St. Louis, MO). Arsenic pentoxide (APO) (As_2O_5, arsenate) was purchased from Wako (Osaka, Japan). Both ATO and APO were dissolved in 1 N NaOH at 0.1 M as a stock solution. An inducible nitric oxide synthase (iNOS) inhibitor, 1400W, was purchased from Calbiochem (Merck Biosciences, Darmstadt, Germany).

Cell culture. 293FT cells were cultured in Dulbecco's modified Eagle's medium (Invitrogen, Carlsbad, CA, USA) supplemented with 10% fetal bovine serum. The following four HuH-7-derived cell lines or their parental HuH-7 cells

* Corresponding author. Mailing address: Department of Tumor Virology, Okayama University Graduate School of Medicine, Dentistry, and Pharmaceutical Sciences, 2-5-1, Shikata-cho, Okayama 700-8558, Japan. Phone: 81 86 235 7385. Fax: 81 86 235 7392. E-mail: nkato@md.okayama-u.ac.jp.

▽ Published ahead of print on 24 December 2008.

were cultured in Dulbecco's modified Eagle's medium with 10% fetal bovine serum as described previously (25): O cells, harboring a replicative genome-length HCV-O RNA (O strain of genotype 1b) (25); OR6 cells, harboring the genome-length HCV-O RNA with luciferase as a reporter (25); sO cells, harboring the subgenomic replicon RNA of HCV-O (31); and RSc cured cells, which cell culture-generated HCV-JFH1 (JFH1 strain of genotype 2a) (58) could infect and effectively replicate in (2, 3). The O, OR6, and sO cells were maintained in the presence of G418 (300 μg/ml Geneticin; Invitrogen).

RNA interference. Oligonucleotides with the following sense and antisense sequences were used for the cloning of short hairpin RNA (shRNA)-encoding sequences targeted to PML (56) in a lentiviral vector: 5′-GATCCCCAGATGC AGCTGTATCCAAGTTCAAGAGACTTGGATACAGCTGCATCTTTTTTG GAAA-3′ (sense) and 5′-AGCTTTTCCAAAAAAGATGCAGCTGTATCCAA GTCTCTTGAACTTGGATACAGCTGCATCTGGG-3′ (antisense). These oligonucleotides were annealed and subcloned into the BglII-HindIII site, downstream from an RNA polymerase III promoter of pSUPER (8), to generate pSUPER-PMLi. To construct pLV-PMLi, the BamHI-SalI fragments of pSUPER-PMLi were subcloned into the BamHI-SalI site of pRDI292, an HIV-1-derived self-inactivating lentiviral vector containing a puromycin resistance marker allowing for the selection of transduced cells (7). pLV-Chk2i was described previously (3).

Lentiviral vector production. The vesicular stomatitis virus (VSV) G-pseudotyped HIV-1-based vector system has been described previously (42). The lentiviral vector particles were produced by transient transfection of the second-generation packaging construct pCMV-ΔR8.91 (1, 71) and the VSV G envelope-expressing plasmid pMDG2 as well as pRDI292 into 293FT cells with FuGene6 (Roche Diagnostics, Mannheim, Germany).

HCV infection experiments. The supernatants was collected from cell culture-generated HCV-JFH1 (58)-infected RSc cells (2, 3) at 5 days postinfection and stored at −80°C after filtering through a 0.45-μm filter (Kurabo, Osaka, Japan) until use. For infection experiments with HCV-JFH1 virus, RSc cells (1×10^5 cells/well) were plated onto six-well plates and cultured for 24 h. We then infected the cells with 50 μl (equivalent to a multiplicity of infection of 0.05 to 0.1) of inoculum. The culture supernatants were collected at 97 h postinfection, and the levels of the core protein were determined by enzyme-linked immunosorbent assay (Mitsubishi Kagaku Bio-Clinical Laboratories, Tokyo, Japan). Total RNA was isolated from the infected cellular lysates using an RNeasy minikit (Qiagen, Hilden, Germany) for quantitative reverse transcription-PCR (RT-PCR) analysis of intracellular HCV RNA. The level of intracellular HCV RNA in the RSc cells was $>10^6$ copies/μg total RNA at 4 days postinfection.

Quantitative RT-PCR Analysis. The quantitative RT-PCR analysis for HCV RNA was performed by real-time LightCycler PCR (Roche) as described previously (25). We used the following forward and reverse primer sets for the real-time LightCycler PCR: PML, 5′-GAGGAGTTCCAGTTTCTGCG-3′ (forward), 5′-GCGCCTGGCAGATGGGGCAC-3′ (reverse); β-actin, 5′-TGACGG GGTCACCCACACTG-3′ (forward), 5′-AAGCTGTAGCCGCGCTCGGT-3′ (reverse); HCV-O, 5′-AGAGCCATAGTGGTCTGCGG-3′ (forward), 5′-CTT TCGCGACCCAACACTAC-3′ (reverse); and HCV-JFH1, 5′-5′-AGAGCCAT AGTGGTCTGCGG-3′ (forward), 5′-CTTTCGCAACCCAACGCTAC-3′ (reverse).

Western blot analysis. Cells were lysed in buffer containing 50 mM Tris-HCl (pH 8.0), 150 mM NaCl, 4 mM EDTA, 1% Nonidet P-40, 0.1% sodium dodecyl sulfate, 1 mM dithiothreitol, and 1 mM phenylmethylsulfonyl fluoride. Supernatants from these lysates were subjected to sodium dodecyl sulfate-polyacrylamide gel electrophoresis, followed by immunoblot analysis using anti-PML (A301-168A-1; Bethyl Laboratories, Montgomery, TX), anti-Chk2 (DCS-273; Medical & Biological Laboratories, MBL, Nagoya, Japan), anti-HCV core (CP-9 and CP-11; Institute of Immunology, Tokyo, Japan), anti-HCV NS5A (no. 8926; a generous gift from A Takamizawa, The Research Foundation for Microbial Diseases of Osaka University, Japan), anti-signal transducer and activator of transcription 3 (anti-STAT3) (BD Bioscience, San Jose, CA), anti-phospho-STAT3 (Tyr705) (Cell Signaling Technology, Danvers, MA) anti-poly(ADP-ribose) polymerase 1 (anti-PARP-1) (C-2-10; Calbiochem), or anti-β-actin antibody (Sigma).

MTT assay. HuH-7 or O cells (5×10^3 cells/well) were plated onto 96-well plates and cultured for 24 h. The cells were treated with ATO, APO, or NaOH for 24, 48, or 72 h and then subjected to the colorimetric 3-(4,5-dimethylthiazol-2-yl)-2,5-diphenyltetrazolium bromide (MTT) assay according to the manufacturer's instructions (cell proliferation kit I; Roche). The absorbance was read using a microplate reader (model 2550; Bio-Rad Laboratories, Hercules, CA) at 550 nm with a reference wavelength of 690 nm.

RL assay. OR6 cells (1.5×10^4 cells/well) were plated onto 24-well plates and cultured for 24 h. The cells were treated with each reagent for 72 h and then subjected to the *Renilla* luciferase (RL) assay according to the manufacturer's instructions (Promega, Madison, WI). A Lumat LB9507 luminometer (Berthold, Bad Wildbad, Germany) was used to detect RL activity.

FL assay. Plasmids were transfected into O cells (2×10^4 cells/well in 24-well plates) using FuGene6 and cultured for 24 h. The cells were treated with or without 1 μM ATO for 24 h, and then firefly luciferase (FL) assays were performed according to the manufacturer's instructions (Promega).

Immunofluorescence and confocal microscopic analysis. Cells were fixed in 3.6% formaldehyde in phosphate-buffered saline (PBS), permeabilized in 0.1% NP-40 in PBS at room temperature, and incubated with anti-PML antibody (PM001; MBL) at a 1:300 dilution in PBS containing 3% bovine serum albumin at 37°C for 30 min. They were then stained with fluorescein isothiocyanate-conjugated anti-rabbit antibody (Jackson ImmunoResearch, West Grove, PA) at a 1:300 dilution in PBS containing bovine serum albumin at 37°C for 30 min, followed by staining with 4′,6-diamidino-2-phenylindole (DAPI) at room temperature for 15 min. Following extensive washing in PBS, the cells were mounted on slides using a mounting medium of 90% glycerin–10% PBS with 0.01% *p*-phenylenediamine added to reduce fading. Samples were viewed under a confocal laser-scanning microscope (LSM510; Zeiss, Jena, Germany).

Measurement of intracellular O_2^- and H_2O_2 production. The intracellular superoxide anion radical (O_2^-) levels were measured with an oxidation-sensitive fluorescent probe, dihydroethidium (DHE) (Invitrogen Molecular Probes), that is highly selective for detection of O_2^- among reactive oxygen species (ROS). DHE is cell permeative and reacts with O_2^- to form ethidium, which in turn intercalates in DNA, thereby exhibiting a red fluorescence. The intracellular hydrogen peroxide (H_2O_2) levels were measured with another oxidation-sensitive fluorescent probe dye, 6-carboxy-2′,7′-dichlorodihydrofluorescein diacetate (carboxy-H_2DCFDA) (Invitrogen Molecular Probes). Carboxy-H_2DCFDA was intracellularly deacetylated with esterase and further oxidized with peroxidase to the fluorescent 2′,7′-dichlorodihydrofluorescein (DCF). The ATO- or BSO-treated O cells were washed with PBS and incubated with 5 μM DHE and 20 μM carboxy-H_2DCFDA in PBS at 37°C for 30 min. Cells were then washed twice with PBS. The DHE or DCF fluorescence intensity was measured using a FACSCalibur flow cytometer. For each sample, 10,000 events were collected. The O_2^- or H_2O_2 levels are indicated as mean fluorescence intensities, which were determined with the CellQuest software (BD Bioscience).

Detection of intracellular glutathione. Intracellular glutathione levels were analyzed using CellTracker Green (5-chloromethylfluorescein diacetate [CMFDA]; Molecular Probes, Invitrogen). CMFDA is a membrane-permeative dye used to determine intracellular glutathione levels. Cytoplasmic esterase converts the nonfluorescent CMFDA to the fluorescent 5-chloromethylfluorescein (CMF), which can then react with glutathione. The excitation peak is at 492 nm, and the fluorescence emission peak is at 517 nm. O cells treated with 1 μM ATO for 72 h were washed with PBS and incubated with 5 μM CMFDA at 37°C for 30 min. The CMF fluorescence intensity was measured using a FACSCalibur flow cytometer. For each sample, 10,000 events were collected. The glutathione levels are given as the relative mean fluorescence intensities, which were determined with CellQuest software.

RESULTS

ATO inhibits HCV RNA replication. First, we quantitatively examined the effect of ATO on the HCV RNA replication in HuH-7-derived O cells harboring a replicative genome-length HCV-O RNA (25). We found that submicromolar concentrations of ATO markedly inhibited genome-length HCV-O RNA replication in the O cells at 72 h after administration (Fig. 1A). The 50% effective concentration (EC_{50}) of ATO required for inhibition of genome-length HCV-O RNA replication was 0.19 μM (Fig. 1A). Consistent with this finding, the expression levels of the HCV core and NS5A proteins were also significantly decreased in the cell lysates of O cells treated with ATO for 72 h (Fig. 1B). In addition, ATO markedly inhibited the replication of the subgenomic replicon RNA (31), with an EC_{50} of 0.48 μM at 72 h after the treatment (Fig. 1C). We next examined the effect of ATO on HCV reproduction by HCV-JFH1 infection (58). The results revealed that ATO significantly inhibited the intracellular RNA replication of HCV-

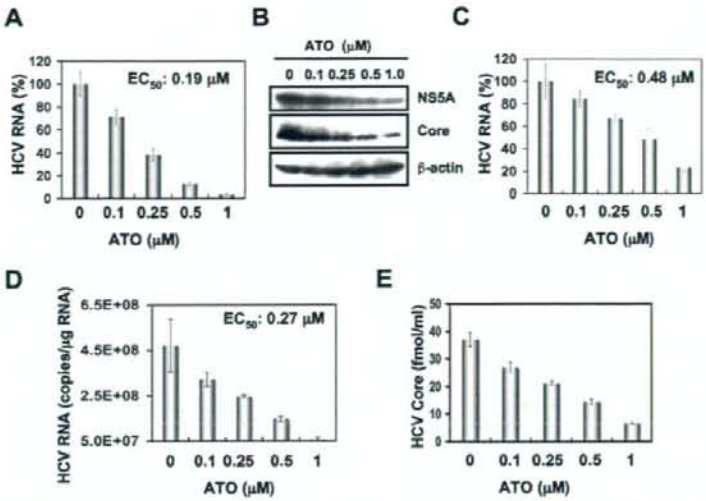

FIG. 1. Inhibition of HCV RNA replication by ATO. (A) The level of genome-length HCV RNA in O cells after the treatment with ATO was monitored by real-time LightCycler PCR. Experiments were done in triplicate and, bars represent the mean percentage of HCV RNA. Error bars indicate standard deviations. (B) HCV core and NS5A protein expression levels in O cells after treatment with ATO. The results of Western blot analysis of cellular lysates with anti-HCV core, anti-HCV NS5A, or anti-β-actin antibody in O cells at 72 h after treatment with ATO at the indicated concentration are shown. (C) The level of subgenomic replicon RNA was monitored by real-time LightCycler PCR. Results from three independent experiments conducted as described for panel A are shown. (D) The level of intracellular genome-length HCV-JFH1 RNA was monitored by real-time LightCycler PCR. RSc cells were pretreated with the indicated concentration of ATO for 13 h, followed by inoculation of the HCV-JFH1 virus, and then the infected cells were further incubated with ATO for 97 h. Results from three independent experiments conducted as described for panel A are shown. (E) The levels of the core protein in the culture supernatants treated as described for panel D were determined by enzyme-linked immunosorbent assay. Experiments were done in triplicate, and bars represent the mean core protein levels.

JFH1, with an EC_{50} of 0.27 μM, as well as the release of core protein into the culture supernatants in HuH-7-derived RSc cells at 97 h after inoculation of the HCV-JFH1 virus (Fig. 1D and E). Thus, we have demonstrated for the first time that ATO can inhibit the reproduction of HCV and particularly HCV RNA replication.

Effect of APO on HCV replication. Arsenic is known to exist in two oxidation states, As(III) in ATO and As(V) in APO. As ATO in the lower valence state has been reported to be more toxic than APO (48), we compared their anti-HCV activities using an OR6 assay system, which was recently developed as a luciferase reporter assay system for monitoring genome-length HCV RNA replication in HuH-7-derived OR6 cells (Fig. 2A) (25). The results showed that APO could not strongly suppress HCV replication at submicromolar concentrations, while ATO strongly inhibited it, with an EC_{50} of 0.33 μM (Fig. 2B and C), indicating that ATO has unique anti-HCV activity. In this context, it is relevant that the expression level of HCV core protein was also remarkably decreased in the cell lysates of O cells treated with ATO, but not those treated with APO, for 72 h (Fig. 2D). Thus, APO seems to be a useful negative probe to clarify the mechanism of the anti-HCV activity of ATO.

ATO does not affect cell growth at submicromolar concentrations. ATO has been reported to induce apoptosis (11, 14, 20, 21, 26–28, 33, 48, 66). Therefore, such an ATO-induced apoptosis may be involved in the anti-HCV activity. To test this possibility, we examined the effect of ATO or APO at various concentrations on cell proliferation by colorimetric MTT assay. In this context, we demonstrated that ATO did not affect the cell proliferation of O cells or the parental HCV-negative HuH-7 cells at submicromolar concentrations (Fig. 3A and E). In contrast, 4 or 8 μM ATO significantly inhibited cell proliferation (Fig. 3B and F). Similarly, APO did not affect the cell proliferation at less than 2 μM (Fig. 3C and D). Consistent with the above results, ATO-treated O cells exhibited normal growth rates and cell viabilities, at least at 1 μM for 72 h (Fig. 3G). Furthermore, we did not observe the cleavage of PARP-1, which is known to be an important substrate for activated caspase 3, in O cells treated with 1 μM ATO at least until 72 h (Fig. 3H), indicating that 1 μM ATO did not induce apoptosis in O cells. Thus, we concluded that the anti-HCV activity was independent of ATO-induced apoptosis or cell toxicity, at least at submicromolar concentrations.

PML and Chk2 are dispensable for the anti-HCV activity of ATO. Since PML is known to be a target of ATO (70), we first examined the subcellular localization of PML in O cells treated with either 1 μM ATO or 1 μM APO for 72 h by means of an anti-PML antibody (PM001; MBL) that can recognize most of the PML splicing variants and is useful for immunofluorescence analysis. The results showed that PML was localized predominantly in punctate nuclear speckles termed PML-NBs in control O cells (Fig. 4A). Interestingly, we noticed that some nuclear PML, but not all, disappeared and was translocated into discrete cytoplasmic bodies in the O cells treated with 1 μM ATO (Fig. 4A). We also observed cytoplasmic translocation of PML in the O cells treated with 1 μM APO for 72 h (Fig. 4A). Furthermore, we observed a similar cytoplasmic translocation of PML in the HCV-negative 293FT or HeLa

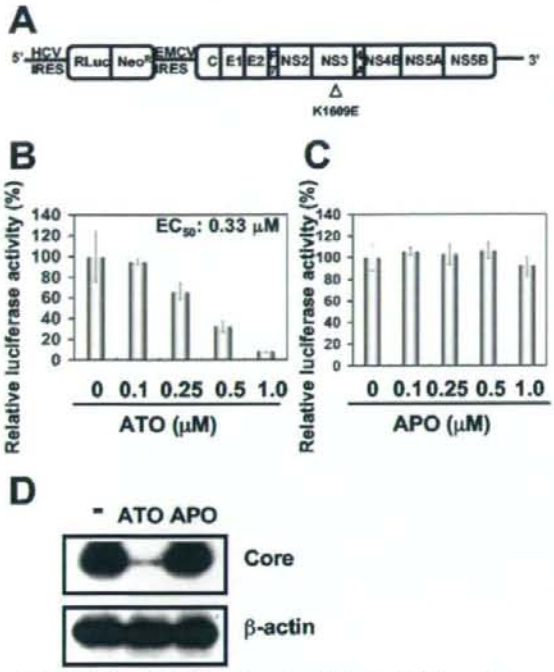

FIG. 2. Effect of APO on HCV replication. (A) Schematic representation of genome-length HCV RNA encoding the RL gene as a reporter (ORN/C-5B/KE RNA) replicated in OR6 cells. The RL is expressed as a fusion protein with neomycin phosphotransferase (Neo^R). The position of an adaptive mutation, K1609E in NS3, is indicated by an open triangle. (B) Effect of ATO on genome-length HCV RNA replication. At 72 h after treatment of OR6 cells with ATO at the indicated concentrations, the replication level of HCV RNA was monitored by the RL assay. The relative RL activity is shown. The results shown are means from three independent experiments. Error bars indicate standard deviations. (C) Effect of APO on genome-length HCV RNA replication. At 72 h after treatment of OR6 cells with APO at the indicated concentrations, the replication level of HCV RNA was monitored by the RL assay as described for panel B. (D) HCV core protein expression level in O cells after treatment with either ATO or APO. The results of Western blot analysis of cellular lysates with anti-HCV core or anti-β-actin antibody in O cells at 72 h after treatment with either 1 μM ATO or 1 μM APO are shown.

cells after the treatment with ATO (data not shown). Thus, we concluded that the cytoplasmic translocation of PML after the treatment with ATO was not associated with anti-HCV activity. Next, Western blot analysis to compare PML expression in the lysates of O cells treated with 1 μM ATO or 1 μM APO for 72 h was performed using another anti-PML antibody, A301-168A-1 (a gift from Bethyl Laboratories), which can recognize the longest isoform, PML I, but not shorter PML isoforms such as PML VI and which has been proven useful for Western blot analysis. Consistent with the previous finding that ATO promotes PML degradation (70), the expression level of the PML I protein was lower in the ATO-treated O cells than in the APO-treated O cells (Fig. 4B), suggesting that PML degradation by ATO is associated with anti-HCV activity. To further examine whether PML is directly involved in the anti-HCV activity of ATO, we used lentiviral vector-mediated RNA interference to stably knock down PML in the O cells. To express an shRNA targeted to all PML isoforms (56), we used the VSV G-pseudotyped HIV-1-based vector system (1, 42, 71). We used the puromycin-resistant pooled cells at 10 days after the lentiviral transduction in this experiment. Immunofluorescence and Western blot analysis demonstrated a very effective knockdown of PML in the O cells (Fig. 4C and D). We quantitatively examined the level of HCV RNA in the PML knockdown O cells treated with or without either 1 μM ATO (Fig. 4E) or 1 μM APO (Fig. 4F) for 72 h. The results showed that the replication level of genome-length HCV-O RNA in the untreated PML knockdown cells was similar to that in control cells (Fig. 4E), suggesting that PML is dispensable in HCV RNA replication. Importantly, ATO effectively inhibited the HCV RNA replication in both the PML knockdown cells and control cells compared with that of the APO-treated cells (Fig. 4E and F). Thus, we concluded that PML was dispensable for the anti-HCV activity of ATO. Since the Chk2 checkpoint kinase has recently been implicated in ATO-induced apoptosis and in association with PML (27, 63, 64, 66), we examined the anti-HCV activity in the ATO-treated Chk2 knockdown O cells (3). As we previously described, Western blot analysis demonstrated very effective knockdown of Chk2 in O cells (Fig. 4G). Accordingly, we examined the level of HCV RNA in Chk2 knockdown cells treated with or without either 1 μM ATO (Fig. 4H) or 1 μM APO (Fig. 4I) for 72 h. Consistent with our recent finding that Chk2 is required for HCV RNA replication, the replication of genome-length HCV RNA in the untreated Chk2 knockdown cells was remarkably suppressed (Fig. 4H). However, ATO strongly inhibited the HCV RNA replication in the Chk2 knockdown cells compared with that in the APO-treated Chk2 knockdown cells (Fig. 4H and I), suggesting that Chk2 is not implicated in the anti-HCV activity of ATO.

Effect of ATO on the stress-signaling pathways. To date, the focus has been on PML and PML-retinoic acid receptor α as major targets of ATO (70). On the other hand, arsenic has been reported to modulate other cell-signaling pathways, especially stress-responsive transcription factors, such as nuclear factor κB (NF-κB), activator protein 1 (AP-1), and STAT3 (12, 37, 38, 62). Therefore, we examined the involvement of several stress-responsive pathways in the anti-HCV activity of ATO by luciferase-based reporter assays or Western blot analysis using an antibody which specifically recognizes STAT3 phosphorylated at tyrosine 705. Although it has been reported that ATO inhibited the NF-κB signaling pathway through a direct interaction with IKKβ at a high concentration (more than 10 μM) (29), neither 1 μM ATO nor 1 μM APO affected the endogenous NF-κB transcriptional activity in the present study (Fig. 5A and B). Conversely, ATO at least slightly stimulated mitogen-activated protein kinase kinase kinase (MEKK)-mediated NF-κB activation (Fig. 5A and B). Since NF-κB activation has been shown to stimulate HCV replication (60), the NF-κB pathway would seem not to be essential for the anti-HCV activity of ATO. Next, regarding the AP-1 signaling pathway, both ATO and APO are known to activate c-Jun N-terminal kinase (JNK) (45). Importantly, there was no stimulation of JNK activity at a dose below 30 μM (45). In fact, 50 μM ATO but not 50 μM APO strongly stimulates AP-1 activity by in-